LBNL-38942
UC-401
Preprint

ERNEST ORLANDO LAWRENCE
BERKELEY NATIONAL LABORATORY

Crossed-Beam Reaction of Carbon Atoms with Hydrocarbon Molecules II: Chemical Dynamics of n-C_4H_3 Formation from Reaction of $C(^3P_j)$ with Methylacetylene, CH_3CCH (X^1A_1)

R.I. Kaiser, D. Stranges, Y.T. Lee, and A.G. Suits
Chemical Sciences Division

June 1996
Submitted to
Journal of Chemical Physics

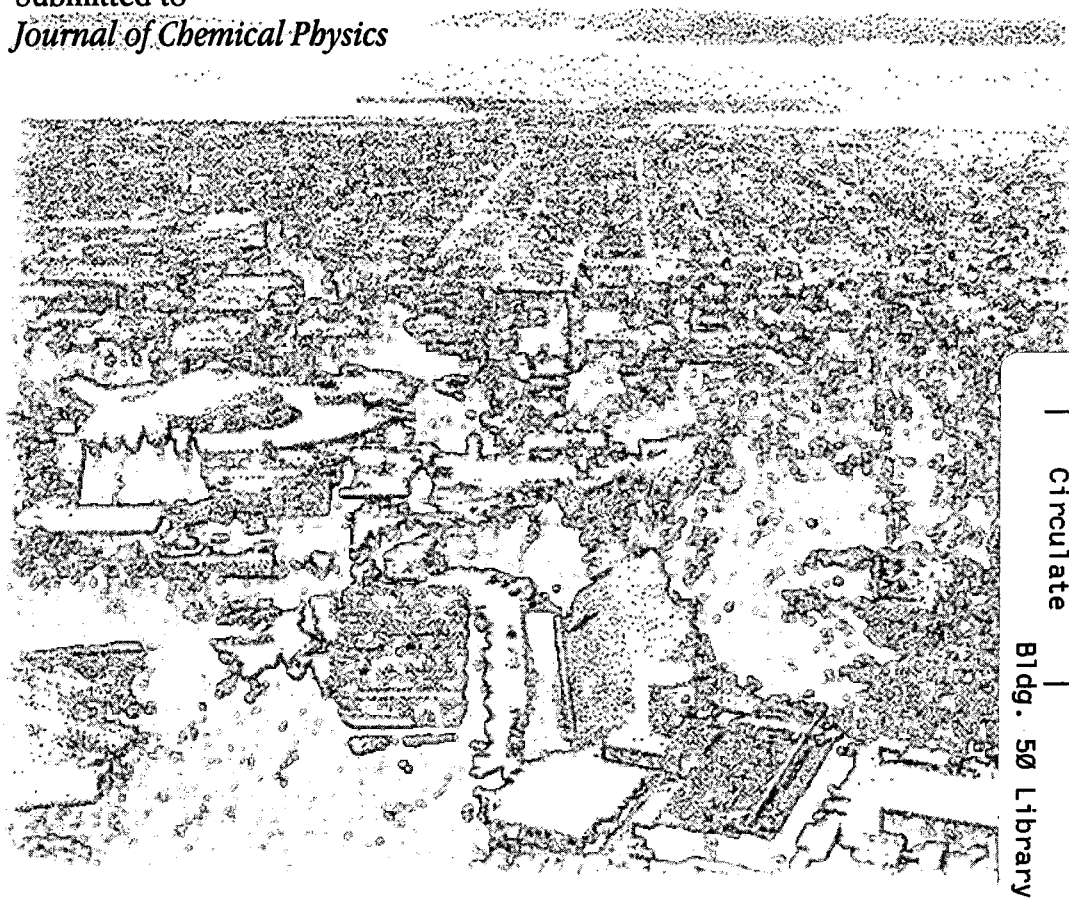

DISCLAIMER

LBNL-38942
UC-401

Crossed-Beam Reaction of Carbon Atoms with Hydrocarbon Molecules II: Chemical Dynamics of n-C_4H_3 Formation from Reaction of $C(^3P_j)$ with Methylacetylene, CH_3CCH (X^1A_1)

R.I. Kaiser,[1] D. Stranges,[1,2] Y.T. Lee,[3] and A.G. Suits[1*]

[1]Department of Chemistry, University of California, Berkeley, and Chemical Sciences Division, Ernest Orlando Lawrence Berkeley National Laboratory, University of California, Berkeley, California 94720
[2]Present Address: Dipartimento Chimica, Universita La Sapienza, Piazzale A. Moro 5, 00185 Rome, Italy
[3]Academia Sinica, Nankang, Taipei 11529, Taiwan

June 1996

*To whom correspondence should be addressed.

This work was supported by the Director, Office of Energy Research, Office of Basic Energy Sciences, Chemical Sciences Division, of the U.S. Department of Energy under Contract No. DE-AC03-76SF00098.

ABSTRACT

The reaction between ground state carbon atoms, $C(^3P_j)$, and methylacetylene, CH_3CCH (X^1A_1), was studied at average collision energies of 20.4 and 33.2 kJmol^{-1} using the crossed molecular beams technique. Product angular distributions and time-of-flight spectra of C_4H_3 at m/e = 51 were recorded. Forward-convolution fitting of the data yields weakly polarized center-of-mass angular flux distributions isotropic at lower, but forward scattered with respect to the carbon beam at a higher collision energy. The translational energy flux distributions peak at 30 - 60 kJmol^{-1} and show an average fractional translational energy release of 22 to 30 %. This maximum energy release as well as the angular distributions are consistent with the formation of the n-C_4H_3 radical in its electronic ground state. Reaction dynamics inferred from the distributions indicate that the carbon atom attacks the π-orbitals of the methylacetylene molecule via a loose, reactant like transition state located at the centrifugal barrier. The initially formed triplet 1-methylpropendiylidene complex rotates in a plane almost perpendicular to the total angular momentum vector around the B\C-axes and undergoes [2,3]-hydrogen migration to triplet 1-methylpropargylene. Within 1 - 2 ps, the complex decomposes via C-H-bond cleavage to n-C_4H_3 and atomic hydrogen. The exit transition state is found to be tight and located at least 30 - 60 kJmol^{-1} above the products. The explicit identification of the n-C_4H_3 radical under single collision conditions represents a further example of a carbon-hydrogen exchange in reactions of ground state carbon atoms with unsaturated hydrocarbons. This channel opens a versatile pathway to synthesize extremely reactive hydrocarbon radicals relevant to combustion processes as well as interstellar chemistry.

I. INTRODUCTION

The interstellar medium (ISM) consists of gas and sub-μm sized grain particles with averaged number densities of 1 H atom cm^{-3} and 10^{-11} grains cm^{-3}. Its chemical composition is dominated by hydrogen and helium (H:He ≈ 1: 0.1), whereas the biogenic elements oxygen, carbon, and nitrogen contribute ≈ 0.001 relative to atomic hydrogen [1-2]. Comprising approximately 99% neutrals and 1% ions, interstellar radicals, atoms, and molecules are not distributed homogeneously, but primarily localized in interstellar clouds as well as outflow of carbon stars [1-2]. Diffuse (hot) clouds hold number densities n up to 100 molecules cm^{-3} and mean translational temperatures T of about 100 K, whereas in dense (cold, dark, molecular) clouds typical scenarios range between n = 10^2 - 10^6 cm^{-3} and T = 10 - 40 K. Molecules in the outflow of carbon stars contributes only a minor amount, but temperatures can rise up to 4000 K [3], and a more complex chemistry is expected as compared to interstellar clouds.

Since the average kinetic energy of the interstellar species is confined to typically 0.8 $kJmol^{-1}$ (diffuse clouds) and 0.08 $kJmol^{-1}$ (dark clouds), gas phase reactions under thermodynamic equilibrium conditions must have little or no barriers and involve only two body collisions. Ternary encounters occur only once in a few 10^9 years, and can be excluded considering mean interstellar cloud lifetimes of 10^6 years [4]. The first chemical equilibrium models of interstellar chemistry satisfy these criteria and focus on ion-molecule reactions, radiative associations, as well as dissociative recombination between cations and electrons to advance interstellar chemistry [5, 6]. This approach, however, involves reaction chains with subsequent collisions, and often cannot reproduce observed structural isomer ratios as well as number densities for example of C_3H and C_3H_2 [7]. The inclusion of alternative, one step, exothermic neutral-neutral reactions into chemical models of the circumstellar envelope surrounding the carbon star IRC+10216 and the dark cloud TMC-1 occurred only gradually [8-16]. However, the *ad hoc* postulation of spin conservation

and simple thermochemistry clearly demonstrate the urgency of systematic laboratory examinations probing detailed chemical dynamics and reaction products of neutral-neutral encounters.

Very recently, these studies were initiated investigating exothermic atom-molecule reactions of atomic carbon in its ^3P_j electronic ground state with unsaturated hydrocarbons via the crossed beam technique as a potential source tri carbon hydride and the propargyl radical [7, 17]:

(1) $$C(^3P_j) + C_2H_2(X^1\Sigma_g^+) \rightarrow l/c(?)\text{-}C_3H + H(^2S_{1/2})$$

(2) $$C(^3P_j) + C_2H_4(X^1A_g) \rightarrow C_3H_3(X^2B_1) + H(^2S_{1/2}).$$

The explicit identification of this carbon-hydrogen exchange channel opens a versatile synthetic pathway to carbon bearing species. Analogous to (1), reaction of $C(^3P_j)$ with methylacetylene, CH_3CCH, is expected to yield hitherto unobserved interstellar C_4H_3 isomer(s):

(3) $$C(^3P_j) + CH_3CCH(X^1A_1) \rightarrow C_4H_3 + H.$$

Its prospective methylacetylene precursor and atomic carbon have been widely observed in the molecular clouds OMC-1 [18] and TMC-1 [19] with fractional abundances relative to hydrogen between $4*10^{-9}$ and $6.3*10^{-9}$. Likewise, methylacetylene [20-22] as well as C_4H_3 isomers are included in a photochemical model of Titan, Jupiter, and Saturn [23-24]. The authors postulate C_4H_3 formation via three body recombination

(4) $$H + C_4H_2 + M \rightarrow M + C_4H_3,$$

although cosmic ray produced carbon atoms survive the reducing atmospheres [25] and might react via (3).

Besides its potential interstellar relevance, a scavenged C_4H_3 isomer in acetylene/oxygen flames [26] is expected to play a significant role in formation of the first aromatic ring in sooting combustion flames. Wang et al. postulated a stepwise ring growth initiated by (5) or (6) to the phenyl radical or benzyne [27]

(5) $$n\text{-}C_4H_3 + C_2H_2 + M \rightarrow C_6H_5 + M$$

(6) $$n\text{-}C_4H_3 + C_2H_2 \rightarrow C_6H_4 + H,$$

whereas Walsh outlined $i\text{-}C_4H_3$ reacts with only a minor entrance barrier as well [28].

However, no reliable information is available on the mechanism of C_4H_3 radical formation. Miller et al. suggested pathways via (7-10) [29], followed by interconversion of i/n-C_4H_3 (11):

(7) $C_3H_2 + {}^3CH_2 \rightarrow n\text{-}C_4H_3 + H$

(8) $l\text{-}C_3H_3 + CH \rightarrow i/n\text{-}C_4H_3 + H$

(9) $CH_2CHCCH + OH \rightarrow H_2O + i/n\text{-}C_4H_3$

(10) $CH_2CHCCH + H \rightarrow H_2 + i/n\text{-}C_4H_3.$

(11) $i\text{-}C_4H_3 + H \leftrightarrow C_4H_4 \leftrightarrow n\text{-}C_4H_3 + H.$

Alternatively, acetylene dimerization (12) [30-31], recombination with C_2H (13) [32], and thermal decomposition of vinylacetylene intermediates (14) [33-35] might yield C_4H_3:

(12) $2\ C_2H_2 \rightarrow H + i\text{-}C_4H_3$

(13) $C_2H + C_2H_2 \rightarrow i\text{-}C_4H_3$

(14) $CH_2CHCCH \rightarrow i/n\text{-}C_4H_3.$

Although atomic carbon is only a minor species in oxidative flames, it is assumed to contribute significantly to combustion chemistry [36], and the carbon-hydrogen exchange channel (3) could synthesize several C_4H_3 isomers as well as advance diamond synthesis in methylacetylene flames [37].

However, despite the potential astrochemical and combustion relevance, the experimental as well as theoretical characterization of the C_4H_3 PES is far from being complete, Fig. 1. n-C_4H_3 (1a/b) holds the global minimum on the doublet C_4H_3 PES ($\Delta_fH = 486 \pm 3$ kJmol^{-1}) [28, 38-39], followed by a 40 ± 1 kJmol^{-1} less stable iso isomer (2) ($\Delta_fH = 526 \pm 4$ kJmol^{-1}) [28, 38]. The structure of i-C_4H_3 has not yet been resolved. Gay et al. calculated a bent, α-ethinylvinyl carbon skeleton, whereas ESR studies in an argon matrix at 4 K support a linear structure with $^2B_2$ electronic ground state of the butatrienyl radical [40-41]. Very recently, high level *ab initio* calculations at the SCF-CISD(6-311G**) level depict a quasilinear structure (1a) and an interconversion barrier between both bent C_4H_3 conformations (1b) of only 3 kJmol^{-1} [42]. Since the C_4H_3 isomers are extremely reactive, isolation is restricted to a low temperature matrix (n-C_4H_3) or trapping as an 1,3-μ_3-dimetalated cyclic species (M1) as well as 1,3,3-μ_4-trimetalated chain isomer (M2) [43-44].

In this paper, we investigate the detailed chemical dynamics of the atom-neutral reaction of $C(^3P_j)$ with methylacetylene, $CH_3CCH(X^1A_1)$ under single collision conditions at collision energies of 20.4 $kJmol^{-1}$ and 33.2 $kJmol^{-1}$ as provided in crossed molecular beam experiments. The insights into the reaction dynamics disclose precise information on the hitherto unexplored triplet C_4H_4 and doublet C_4H_3 potential energy surface (PES) under well-defined collision energies, and potential exit channel(s) to C_4H_3 isomers.

II. EXPERIMENTAL SETUP AND DATA ANALYSIS

Owing to the high reactivity of prospective open shell products, reactions must be performed under single collision conditions to identify the primary reaction products. These requirements are achieved here using a universal crossed molecular beam apparatus described in ref. [45] in detail. A pulsed supersonic carbon beam was generated via laser ablation of graphite at 266 nm [46]. The 30 Hz, 35-40 mJ output of a Spectra Physics GCR-270-30 Nd:YAG laser is focused onto a rotating carbon rod. Ablated carbon atoms are seeded into neon or helium released by a Proch-Trickl pulsed valve operating at 60 Hz, 80 μs pulses, and 4 atm backing pressure. A four slot chopper wheel mounted 40 mm after the ablation zone selects a 9.0 μs segment of the seeded carbon beam. Table 1 compiles the experimental beam conditions. The pulsed carbon and a continuous methylacetylene beam at 515±10 torr backing pressure pass through skimmers, and cross at 90° in the interaction region of the scattering chamber. Reactively scattered products were detected in the plane of the beams using a rotable detector consisting of a Brink-type electron-impact ionizer [47], quadrupole mass filter, and a Daly ion detector [48] at different laboratory angles in 5.0^0 steps between 5.0^0 and 60.0^0 with respect to the carbon beam. The velocity distribution of the products was recorded using the time-of-flight (TOF) technique [49] choosing a channel width of 7.5 μs. Counting times ranged from 0.5 - 4 h, averaged over several angular scans. The velocity of the supersonic carbon beam was monitored frequently after 2 - 5 angles and minor velocity drifts corrected by adjusting the laser pulse delay within ± 1.5 μs. A

reference angle was chosen at 55^0 and 45^0, respectively, to calibrate fluctuating carbon beam intensities and mass dial settings at the quadrupole controller.

Information on the reaction dynamics is gained by fitting the TOF spectra and the product angular distribution in the laboratory frame using a forward-convolution routine [50-51]. This iterative approach initially guesses the angular flux distribution $T(\theta)$ and the translational energy flux distribution $P(E_T)$ in the center-of-mass system (CM) assuming mutual independence. Laboratory TOF spectra and the laboratory angular distributions were then calculated from these $T(\theta)$ and $P(E_T)$ averaged over a grid of Newton diagrams defining the velocity and angular spread of each beam, detector acceptance angle, and the ionizer length. Best TOF and laboratory angular distributions were archived by iteratively refining adjustable $T(\theta)$ and $P(E_T)$ parameters.

III. RESULTS

A. REACTIVE SCATTERING SIGNAL

Reactive scattering signal was only observed at m/e = 51, i.e. C_4H_3, c.f. Figs. 2 - 5 and Tab. 2. Reaction of carbon with methylacetylene dimers does not contribute the data, since the integrated m/e = 51 signal scales linearly with the CH_3CCH source backing pressure. TOF spectra recorded at m/e = 48 - 50 show identical patterns indicating the signal originates in cracking of the parent in the detector. Energetically accessible channels 2 - 3 to diacetylene (Tab. 2), C_4H_2, are absent within detection limits of our system, and endothermic channels 3 - 4 could not be opened at relative collision energies up to 33.2 $kJmol^{-1}$ applied in our experiments. In addition, no radiative association to C_4H_4 isomers at m/e = 52 or higher masses were observed. Lower molecular weight products bearing two or three carbon atoms (exothermic channels 6 - 12) could not be verified yet. Their detection suffers from the high background level via methylacetylene fragmentation in the detector. Upper limits of 40 % (channel 6-8), 60 % (channel 9), 10 % (channel 10), 40 % (channel 11), and 80 % (channel 12) relative to m/e = 51 signal were derived.

B. LABORATORY ANGULAR DISTRIBUTION (LAB) AND TOF SPECTRA

Figs. 2 and 3 display the most probable Newton diagrams of the title reaction as well as the laboratory angular (LAB) distributions of the C_4H_3 product at collision energies of 20.4 and 33.2 kJmol^{-1}, respectively. Both LAB distributions peak close to the CM angles at 53.5^0 and 46.2^0 and show a slightly forward peaking distribution at higher collision energy. This behavior suggests indirect reaction dynamics via a long-lived C_4H_4 complex with a lifetime exceeding (20.4 kJmol^{-1}) or comparable to its rotational period (33.2 kJmol^{-1}, osculating complex). Since the enthalpy of formation of low lying C_4H_3 isomers differs only by about 30-50 kJmol^{-1}, Fig. 1, the nature of the C_4H_3 solely based on limiting circles is not possible. The maximum scattering range of isomers (1)-(8) falls within 8^0, and individual limit circles are blurred out due to the velocity spread of the carbon beam (Tab. 1). However, the scattering range of the m/e = 51 product allows us to eliminate isomer (9) and the endothermic channel to isomer (10). Further, the large width of the laboratory angular distribution of at least 60^0 and the C_4H_3 + H product mass ratio of 51 indicates that the averaged translational energy release $\langle E_T \rangle$ is large and that the center-of-mass translational energy distributions $P(E_T)$s peak well away from zero, c.f. III.C.

C. CENTER-OF-MASS TRANSLATIONAL ENERGY DISTRIBUTION, $P(E_T)$

Figs. 6 and 7 present the translational energy distributions $P(E_T)$ and angular distributions $T(\theta)$ in the center-of-mass frame. Both LAB distributions and TOF data were fitted with a single $P(E_T)$ extending to a maximum translational energy release E_{max} of 110 - 170 kJmol^{-1} and 225 - 255 kJmol^{-1}, respectively. If the energetics of distinct isomers are well separated, E_{max} can be used to identify individual C_4H_3 isomers. The maximal translational energy releases, i.e. the sum of the reaction exothermicity and relative collision energy, were already presented in Fig. 2 and 3 with a reasonable approximation of rotationally and vibrationally cold methylacetylene molecules prepared in the supersonic expansion. The production of the n-C_4H_3 isomer at 33.2 kJmol^{-1} is evident by comparing the theoretical and experimental high energy cutoff of $P(E_T)$ with

E_{max}(exp.; 33.2 kJmol^{-1}) = 225 - 255 kJmol^{-1} vs. E_{max}(theor.; 33.2 kJmol^{-1}) = 226 ± 7 kJmol^{-1}. Formation of the 40 kJmol^{-1} less stable iso isomer can be rejected, since the maximum energy release is restricted to 186 kJmol^{-1}. Based entirely on the high energy cutoff, the reactive scattering product at lower collision energy is hard to identify, since all C_4H_3 isomers (2) - (6) fall within the E_{max} range. Due to the internal excitation of the C_4H_3 product, even (1) cannot be ruled out, c.f. III.D.

Besides identification of structural isomers, the most probable translational energy yields the order-of-magnitude of the barrier height in the exit channel. Both $P(E_T)$s peak away from zero as expected from the LAB distributions and depict a broad plateau between 30-60 kJmol^{-1}. A exit barrier is further implied by the large fraction of energy channeled into translational motion of the n-C_4H_3 and H products, i.e. 22 ± 5 % and 30 ± 3 % at lower and higher collision energy, respectively. These findings suggest a tight transition state with a significant change in electronic structure as the C_4H_4 complex decomposes.

D. CENTER-OF-MASS ANGULAR DISTRIBUTIONS, T(θ)

At lower collision energy, T(θ) is isotropic and symmetric around π/2 implying that either the fragmenting C_4H_4 holds a lifetime longer than its rotational period τ_r or that the exit transition state is symmetric [54-55]. With increasing collision energy, the center-of-mass angular distribution peaks forward with respect to the carbon beam. These findings indicate a reduced lifetime of the decomposing C_4H_4 complex and agrees with our suggested osculating complex: a complex formation takes place, but the well depth along the reaction coordinate is too shallow to allow multiple rotations, and the complex decomposes with a random lifetime distribution before one full rotation elapses. Based on the intensity ratio of T(θ) at θ = 0° and 180° of 1.7± 0.1, the identification of the fragmenting complex enables us to use the rotational period of the complex as a molecular clock to estimate its lifetime (c.f. IV.D). To explain the forward-peaking, the

carbon atom and the leaving hydrogen atom must further be situated on opposite sites of the rotation axis of the fragmenting complex.

The weak polarization of all T(θ)s can be explained solely based on total angular momentum conservation and angular momentum disposal [17, 54, 55]. In terms of a classical treatment, the total angular momentum **J** is given by

(15) $$\mathbf{J} = \mathbf{L} + \mathbf{j} = \mathbf{L'} + \mathbf{j'}$$

with the initial and final orbital angular momentum **L** and **L'** perpendicular to the initial and final relative velocity vectors **v** and **v'**, and **j** and **j'** the rotational angular momenta of reactants and products. Since bulk experiments indicate that the reaction of $C(^3P_j)$ with CH_3CCH proceeds within orbiting limits [56] and our relative cross sections rise with decreasing collision energy (III.E), an upper limit of the impact parameter, b_{max}, is determided via the classical capture theory [56, 57]. Approximating the Lennard-Jones coefficient C_6 according to Hirschfelder et al. [58] and using the ionization potentials $E_{C(3Pj)}$ = 11.76 eV, E_{C3H4} = 10.36 eV, and polarizabilities $\alpha_{C(3Pj)} = 1.76*10^{-30}$ m^3, $\alpha_{C3H4} = 6.18*10^{-30}$m^3[52], b_{max} gives rise to b_{max}(20.4 kJmol^{-1}) = 3.8Å and b_{max}(33.2 kJmol^{-1}) = 3.2Å. The maximum orbital angular momentum yields L_{max}(20.4 kJmol^{-1}) = 116$\hbar$ and L_{max}(33.2 kJmol^{-1}) = 125$\hbar$. Since CH_3CCH is produced in a supersonic expansion and j peaks at 2-4$\hbar$ for typical rotational temperatures between 20 and 40 K, **j** contributes less than 2.5% to the total angular momentum **J**, and (15) reduces to:

(16) $$\mathbf{L} \approx \mathbf{J} = \mathbf{L'} + \mathbf{j'}.$$

To justify the weak T(θ) polarizations, **L** and **L'** must be uncoupled with **j'** >> **L'**, and the initial orbital angular momentum becomes the final rotational angular momentum. This weak **L**-**L'** correlation is a direct result of the inability of the departing H atom to carry significant orbital angular momentum. On the other hand, a strong **L**-**L'** correlation would have indicated that the complex decomposed with **L'** ≥ **j'**, but the expected $(\sin\theta)^{-1}$ shaped T(θ) at 20.4 kJmol^{-1} is clearly not observed.

E. FLUX CONTOUR MAPS AND TOTAL RELATIVE CROSS SECTIONS

Figures 8-9 show center-of-mass flux contour maps $I(\theta, E_T) \sim T(\theta) * P(E_T)$ for collision energies at 20.4 and 33.2 kJmol^{-1}. Data at lower collision energy depict a forward-backward symmetric flux profile as expected from the center-of-mass angular distributions. With increasing collision energy, the pronounced forward peaking on the relative velocity vector is evident. Integrating this flux distribution and correcting for the reactant flux as well as relative reactant velocity, we find a total, relative cross section ratio of σ (20.4 kJmol^{-1}) / σ(33.2 kJmol^{-1}) = 1.7 ± 0.4. This finding together with recent bulk experiments [56] suggest a barrier-less, attractive long-range dispersion forces dominating the C - CH_3CCH interaction as well as a loose, reactant-like transition state located at the centrifugal barrier to the triplet C_4H_4 PES at about 3Å.

F. ENERGY PARTITION OF TOTAL AVAILABLE ENERGY

The identification of the n-C_4H_3 isomer allows us to estimate partition of the total available energy, E_{tot}, into product translation, E_{tr}, ≈ $\langle E_T \rangle$. Even if the butatrienyl structure resembles only an inversion transition state, the 3 kJmol^{-1} barrier can be easily overcome at experimental conditions applied here. The quasilinear n-C_4H_3 radical holds the rotational constants A = 10.17 cm^{-1}, B = 0.139 cm^{-1}, and C = 0.137 cm^{-1} and classify it as a highly prolate asymmetric top with asymmetry parameter κ = - 0.9996, Fig. 10. Hence, we approximate the rotational levels to those of a rigid symmetric top [17] using the rotational quantum number J = 116 (E_{coll} = 20.4 kJmol^{-1}) and J = 125 (E_{coll} = 33.2 kJmol^{-1}) c.f. III.D, and calculate the component of the rotational angular momentum about the principal axis K with K = 0 for no rotation about the figure axis, but perpendicular to it, and K ≈ J for a fast rotation about the principal axis, with a slow end-over-end one. Since no data on the K-distributions are available, we use the same procedure as applied for the C(^3P_j) + C_2H_4 system [17] and calculate first the rotational energy assuming K = 0 (''low K approximation''). This gives us the maximal vibrational energy release E_{vib} in the n-C_4H_3 radical. Hereafter, the highest energetically

accessible K states K_{max} are computed assuming E_{vib} = 0 kJmol^{-1} to estimate an upper limit of the product rotational excitation as well as an order of magnitude of the lowest tilt angle α_{min} of the n-C_4H_3 principal inertial axis in respect to **j'** in terms of the classical vector model [17].

The low K approximation yields a nearly constant partitioning of total energy into rotational degrees of freedom at both collision energies, i.e. 21±2 kJmol^{-1} (10±1 %) versus 26±3 kJmol^{-1} (11±2 %). Further, the fraction of the maximum vibrational energy release stays constant within the error limits (68 ± 20 % and 59 ± 10 %; 145 kJmol^{-1} at lower and 133 kJmol^{-1} at higher collision energy) and might suggest a lifetime long enough to randomize the energy into the vibrational modes of the C_4H_4 complex. Finally, even in the limit of zero vibrational excitation of the n-C_4H_3 product and a maximum K value, the principal axis is tilted 73 - 76° with respect to **j'** and clearly demonstrates a predominant end-over-end-rotation of the n-C_4H_3 radical.

IV. DISCUSSION

In this section, we outline feasible reaction pathways on the triplet C_4H_4 PES to produce C_4H_3 isomers (1) - (6) via insertion of the electrophile carbon atoms into the C-H- and C-C-bonds of methylacetylene, addition to two π-molecular orbitals at both distinct carbon atoms, and, finally, addition to two π-orbitals at one carbon atom. The observed CM angular and translational energy distributions are then compared to what is expected based on these channels. Pathways incompatible with experimental data are dismissed. Since no C_4H_4 intermediate fulfills requirements for intersystem crossing [17], the discussion is resticted to the triple tsurface. However, neither *ab initio* nor experimental enthalpies of formations of triplet C_4H_4 isomers are available, and their energetics are approximated based on corresponding triplet C_3H_2 isomers [59-65].

A. C_4H_4 POTENTIAL ENERGY SURFACE

Addition of $C(^3P_j)$ to two perpendicular π-orbitals at the methylacetylene α-C atom (the neighboring carbon atom to the methyl group) yields triplet s-cis/trans 2-methylpropendiylidene (11)/(12), Fig. 11, whereas attack to the β-C atom forms triplet s-trans/cis 1-methylpropendiylidene (13)/(14). Since trans-propendiylidene is energetically favored by about 80 $kJmol^{-1}$ as compared to the cis isomer on the triplet C_3H_2 surface, this difference is adapted to cis (11)/(14) versus trans (12)/(13) isomers. Further, we approximate identical enthalpies of formations of (11)/(14) (Δ_fH = 815 $kJmol^{-1}$) and (12)/(13) (Δ_fH = 735 $kJmol^{-1}$). (13)/(14) undergo [2,1]-H-migration to triplet 1-methylpropadienylidene (15), [2,3]-H-rearrangement to triplet 1-methylpropargylene (16), ring closure to triplet methylcyclopropenylidene (17), or direct C-H-fragmentation to the linear C_4H_3 isomer (5). Two remaining channels are energetically not accessible: H loss of the methyl group yields a 1,3,3-triradical which - if it existed - suffers ring closure to a tri or tetra cycle which is less stable than the already closed channel to (10); the [1,2] methyl group migration to triplet 2-methylpropanediylidyne (19) is endothermic by 150 $kJmol^{-1}$. Similar to (13)/(14), (11)/(12) might react via [2,3] or [2,1] CH_3-migration to (16) and (15), respectively. Besides addition to α-C-atom, $C(^3P_j)$ might add to both α- and β-C-atoms of the methylacetylene molecule, generating methylcyclopropenylidene (17).

Furthermore, $C(^3P_j)$ insertion into the acetylenic C-H- as well as the C-C-single bond might lead to triplet methylpropargylene (16), whereas insertion into the aliphatic C-H-bond of the methyl group forms a triplet carbene (20). The fate of (15)-(17) is governed by C-H-fragmentation and/or H-migration: (17) decomposes via C-H-bond rupture to (4) or (3), then rearranges to triplet methylenecyclopropene (21), which is followed by H-loss to (3) or (6); the only energetically feasible fragmentation of (15) yields C_4H_3 isomer (5), whereas (16) decomposes either to (5) or n-C_4H_3 (1). Finally, (15) might rearrange via hydrogen migration to triplet vinylidenecarbene (22).

The reaction pathway to the identified n-C_4H_3 radical (III. C) can only proceed via hydrogen loss from the CH_3 group of triplet 1-methylpropargylene (16). Here, the preference of the methyl H-atom loss compared to the acetylenic C-H-bond cleavage even at higher collision energy correlates with the ca. 140 kJmol^{-1} weaker aliphatic carbon-hydrogen bond energy and excludes decomposition of (16) to C_4H_3 isomer (5). Additionally, the identification of (16) as the decomposing complex eliminates the possibility the symmetric T(θ) originates from a symmetric complex (III.D), since rotation around any principal axis cannot fulfil this requirement. The remaining question to be solved is the reaction pathway to (16). Insertion of C(^3P_j) into the acetylenic C-H-bond can be rejected, since only a narrow range of impact parameters between 1.19 and 2.24 Å would contribute to reactive scattering signal. The overwhelming contribution of large impact parameters to the capture process up to 3.8 Å was already mentioned in III.D/E. Additionally, no evidence of insertion was found in the crossed beam reaction of C(^3P_j) with unsubstituted acetylene [17] indicating that the symmetry-forbidden insertion into the acetylenic C-H-bond involves a barrier of at least 33.2 kJmol^{-1}. Insertion into the C-C-single bond can be excluded as well: the forward peaking center of mass angular distribution requires the inserted carbon atom and the leaving hydrogen to be located on opposite sides of the rotation axis of fragmenting (16). However, this condition is not satisfied. In addition, hot atom tracer experiments of ^{11}C(^3P_j) with C_2H_6 and even strained cyclobutane rings show a screening of the C-C-bond by hydrogen atoms, and only insertion into C-H-bonds is observed [66]. Therefore, any insertion process can be excluded from the discussion.

Remaining pathways to (16) involve triplet C_4H_4 intermediates (11)-(14). Using the concept of regioselectivity of electrophilic radical attacks on substituted olefines and extending it to alkynes [67], we can eliminate further collision complexes. The framework predicts the radical attack to be directed at the carbon center which holds the highest spin density. Since partial delocalization of the methyl π-group orbitals increases the spin density on the β-C-atom at the expense of the α-position, C(^3P_j) attacks preferentially at the β-C. Additionally, the sterical hindrance of the CH_3 group reduces the cone of acceptance at the α-C-

atom and the range of reactive impact parameters. Both effects together direct the electrophilic carbon addition to (13)/(14). Even if (11) and (12) were formed to a minor extent, rearrangement to (16) would involve a CH_3-group (m = 15) migration which is unfavorable compared to rearrangement of the light H atom to (16) via (12)/(13). Similar arguments eliminate a simultaneous attack of $C(^3P_j)$ to α- and β-C-atom with maximum impact parameters of about 0.6 Å to (17). Both prevailing pathways to (16) via (13) and (14) cannot be discriminated based on our experimental data. The chemical dynamics to alternative C_4H_3 isomers at lower collision energy involve isomers (13)-(15), (17), or (20). The last one can be ruled out, since insertion of $C(^3P_j)$ into the aliphatic C-H-bond does not play a role. Results of crossed beam experiments $C(^3P_j)$ + CH_4 at relative collision energies up to 40 $kJmol^{-1}$ show no reactive scattering signal of insertion into the aliphatic C-H-bond [68]. Therefore - if (2) contributes - hydrogen loss of triplet vinylacetylene (22) represents the only open channel.

B. ROTATION AXIS OF THE TRIPLET 1-METHYLPROPARGYLENE COMPLEX

Conserving the C-C-C-C-plane as a plane of symmetry, the singly occupied p_x and p_z orbitals of the carbon atom might add to the π_x- and π_z-orbitals of the β-C-atom under C_s symmetry on the $^3A''$ surface [17] to form isomers (13)/(14), Fig. 12. This pathway supports a maximum orbital overlap to the C-C-σ- and C-C-π-bond via interaction of p_x with π_x- as well as p_z with π_z-orbitals. Oblique approach geometries are supported as well and open larger impact parameters for the reaction as discussed in III.E. Since $\mathbf{L} \approx \mathbf{j}'$, the four carbon atoms rotate in a plane approximately perpendicular to **L** around the C-axis of the prolate 1-methylpropendiylidene. The consecutive hydrogen shift to 1-methylpropargylene conserves either the symmetry plane (assuming C_s symmetry of (16b) or (16c), Fig. 12) or follows C_1 symmetry (geometry (16a)). Since the adduct still rotates around the C-axis, the added carbon atom in the C4 position and the methyl hydrogens are located on opposite sites of the rotation axis as required to explain the forward-peaking C_4H_3

product with respcet to the carbon beam. This almost in-plane rotation yields extremely low K values as well as a minor **J** component about the figure axis of the 1-methylpropargylene and can be related to dominating low K states populated in the n-C_4H_3 product (III.F).

An alternative $C(^3P_j)$ trajectory under C_1 symmetry on the ^3A surface might induce rotations about the A, B, and C axes of 1-methylpropendiylidene and - after H-migration - of 1-methylpropargylene, but does not support a maximum overlap of both perpendicular p- with π-orbitals. Furthermore, a freely rotating CH_3 group in (16) undermines A-like rotations, since its hydrogen atoms rotate to the same side as the incorporated carbon atom. Hence, the required forward-peaked T(θ) cannot be supplied.

C. LIFETIME OF THE TRIPLET 1-METHYLPROPARGYLENE COMPLEX

The rotational period of the 1-methylpropargylene complex can act as a clock in the molecular beam experiment and can be used to estimate the lifetime τ of the decomposing complex at a relative collision energy of 33.2 kJmol^{-1}. The osculating model relates the intensity ratio of T(θ) at both poles to τ via (19)

(17) $$I(180^0) / I(0^0) = \exp\left(-\frac{t_{rot}}{2\tau}\right)$$

where t_{rot} represents the rotational period with:

(18) $$t_{rot} = 2\pi I_i / L_{max}$$

I_i represents the moment of inertia of the complex rotating around the i-axis, and L_{max} the maximum linear angular momentum. Using the *ab initio* geometries of propargylene and a C-CH_3 distance in (16) of 1.47 Å, we can estimate the rotational period of the methylpropargylene complex: around the A axis we find $t_{rot}(A)$ = 0.01 - 0.02 ps, and around the B/C axis we obtain $t_{rot}(B, C)$ = 1 - 2 ps. Plugging in all data in (19) yields a lifetime of the triplet 1-methylpropargylene complex equal to one rotational period. The absolute value of τ

depends dramatically on the rotation axis, i.e. B, C vs. A. Since reactions with a collisiontime << 0.1 ps follow direct scattering dynamics, the $T(\theta)$ at 33.2 $kJmol^{-1}$ relative collision energy should be strongly forward peaked, if the complex rotated around the A-axis. Our data show only a moderate peaked center-of-mass angular distribution at 33.2 $kJmol^{-1}$ and an isotropic one at 22.4 $kJmol^{-1}$. Therefore, rotation about the A axis can be eliminated as already suggested in IV.B, and end-over-end rotation around the B- or C-axis of (16) takes place. Due to the optimal orbital overlap (IV.B), C-like rotations should dominate. Compared to the forward peaked $T(\theta)$ as found in the crossed beam reaction $C(^3P_j) + C_2H_2 \rightarrow C_3H + H$ at a relative collision energy of 8 $kJmol^{-1}$, the enhanced complex lifetime is a direct consequence of the additional 9 vibrational modes of the CH_3 group. A similar behavior contributes to the increased lifetime of the triplet 1-methylallene complex (crossed beam reaction $C(^3P_j) + C_3H_6 \rightarrow C_4H_6 \rightarrow C_4H_5 + H$ [69]) versus triplet allene (crossed beam reaction $C(^3P_j) + C_2H_4 \rightarrow C_3H_4 \rightarrow C_3H_3 + H$ [17]).

D. EXIT TRANSITION STATE

The partitioning of the total available energy into the translational, rotational, and vibrational degrees of freedom of the n-C_4H_3 radical as well as the collision energy dependent $P(E_T)$ shape reveal information on the exit transition state. The framework of an ideal RRKM system requires that exit channel interactions, i.e. the coupling between the reaction coordinate (translation) and internal motion beyond the critical configuration, must be small. This condition is only fulfilled in loose transition states, implying the reverse reaction of H + n-C_4H_3 to 1-methylpropargylene holds no entrance barrier. As shown in III.C, the exit transition state is located at least 30-60 $kJmol^{-1}$ above the products, indicating that the C-H-bond rupture in triplet 1-methylpropargylene does not follow the patterns of an ideal RRKM system with a loose transition state. On the other hand, Marcus' tight transition state theory quantifies a rising fraction of total available energy into vibration with increasing collision energy, if the decomposing triplet C_4H_4 complex has many

degrees of freedom. Both $P(E_T)$s clearly underline a tight transition state, but within our error limits, a complete energy randomization cannot be proved or disproved. These deviations from the loose transition state are based on dynamical effects during the separation of fragments into products together with a significant geometry change from the triplet 1-methylpropargylene complex. Comparing the bond orders (BO) of n-C_4H_3, Fig. 1 (1a/b) with those of methylpropargylene, Fig. 11 (16a-c), supports this approach: in the case of a propargylene-like, 1-3 diradical (16a), the C-C-bond orders change from two times 2.5 and 1.0 to an acetylenic (BO = 3), olefinic (BO = 2) and shifted aliphatic C-C-bond (BO = 1). If (16) exists as a triplet carbene (16b/c), the conversion of the C-C-single bond located at the carbene center to a partially delocalized C=C-bond increases the bond strength by ca. 250 kJmol^{-1}. Finally, an isotropic $T(\theta)$ distribution as compared to the forward peaked distribution seen in the reaction $C(^3P_j) + C_2H_2 \rightarrow C_3H + H$ (III.D. and [17]) implies the additional modes of the CH_3 group induce the long-lived complex behavior and that the energy randomization in the collision complex might be complete.

E. ALTERNATIVE ISOMERS AT LOWER COLLISION ENERGY

Based on our experimental results, any of the pathways to C_4H_3 isomers (2) - (6) might show additional contributions at lower collision energy. The electron density change of each triplet C_4H_4 complex fragmenting to (3) - (6) suggest a tight transition state as expected from the center of mass translational energy distribution. Since the relative collision energy increases by only 10 kJmol^{-1}, formation of only one isomer of (2) - (6) with no n-C_4H_3 formation is hard to explain. The isotropic center-of-mass angular distribution might open a potential two channel fit of n-C_4H_3 and a second C_4H_3 isomer as well. However, neither transition state frequencies are available, and the experimental data alone cannot resolve this question.

V. IMPLICATIONS TO INTERSTELLAR CHEMISTRY AND COMBUSTION PROCESSES

The crossed beam setup represents a versatile tool to study reaction products as well as chemical dynamics of neutral-neutral reactions relevant to combustion processes and interstellar chemistry under well-defined reactant conditions. Here, the explicit identification of the n-C_4H_3 radical under single collision conditions depicts a third example of the carbon-hydrogen exchange channel in the reaction of $C(^3P_j)$ with unsaturated hydrocarbons studied recently in our lab [7, 17]:

(19) $$C(^3P_j) + C_2H_2\,(X^1\Sigma_g^+) \rightarrow C_3H + H\,(^2S_{1/2})$$

(20) $$C(^3P_j) + C_2H_4\,(X^1A_1) \rightarrow l\text{-}C_3H_3\,(X\,^2B_1) + H\,(^2S_{1/2}).$$

This reaction class presents an alternative to ion-molecule reactions to synthesize carbon-chain molecules in the interstellar medium [7, 17] and strictly excludes the formation of any C_4H_2 isomer via

(21) $$C(^3P_j) + C_3H_4 \rightarrow C_4H_2 + 2\,H$$

as postulated based on thermochemistry and spin conservation [14] underlining the need of systematic laboratory studies to establish a well-defined data base for neutral-neutral reaction products. A rising cross section with decreasing translation energy underlines the potential contribution of these processes in interstellar clouds and should encourage astronomers to search for hitherto undetected C_4H_3 isomers perhaps among unidentified microwave transitions in the spectrum toward the extended ridge of OMC-1. Since deuterated methylacetylenes (CH_3CCD, and CH_2DCCH) were identified in OMC-1 and TMC-1, formation of partially deuterated C_4H_2D is expected to take place as well. Terrestrial based microwave spectra of C_4H_3 radicals could be simply recorded during RF discharges of CH_3CCH/He/CO-mixtures.

Likewise, the identification of the n-C_4H_3 radical under single collision conditions as well as via trapping experiments in oxygen rich hydrocarbon flames [26] validates inclusion of hydrocarbon radicals even in oxidative flames. Further investigations of $C(^3P_j)$ reactions with unsaturated hydrocarbons are in

progress and will supply a new set of reactions as well as products to be incorporated into combustion models.

VI. CONCLUSIONS

The reaction between ground state carbon atoms, $C(^3P_j)$, and methylacetylene, CH_3CCH, was studied at average collision energies of 20.2 and 33.4 $kJmol^{-1}$ using the crossed molecular beam technique. The carbon atom attacks the π-orbitals of the CH_3CCH molecule via a loose, reactant like transition state located at the centrifugal barrier. The highest symmetric approach follows C_s symmetry on the ground state $^3A''$ surface. The initially formed 1-methylpropendiylidene complex rotates in a plane almost perpendicular to the total angular momentum vector **J** around its C-axis and undergoes hydrogen migration to 1-methylpropargylene. Within 1-2 ps, the complex decomposes via hydrogen emission to n-C_4H_3. The exit transition state is found to be tight and located at least 30-60 $kJmol^{-1}$ above the products. The explicit identification of the n-C_4H_3 radical under single collision represents a further example of a carbon-hydrogen exchange in reactions of ground state carbon atoms with unsaturated hydrocarbons. This channel opens a versatile pathway to synthesize extremely reactive hydrocarbon radicals relevant to combustion processes as well as interstellar chemistry.

ACKNOWLEDGMENTS

R.I.K. is indebted the Deutsche Forschungsgemeinschaft for a post-doctoral fellowship. This work was supported by the Director, Office of Energy Research, Office of Basic Energy Sciences, Chemical Sciences Division of the U.S. Department of Energy under Contract No. DE-AC03-76SF00098.

[1] H. Scheffler and H. Elsässer, Physics of the Galaxy and Interstellar Matter (Springer, Berlin, 1988).

[2] C.R. Cowley, An Introduction to Cosmochemistry (Cambridge University Press, Cambridge, 1985).

[3] Z. K. Alksne, A.K. Alksnis, U.K. Dzervitis, Properties of Galactic Carbon Stars (Orbit Book, Malabar, 1991).

[4] W. Schutte, Ph.D. thesis, University of Leiden.

[5] D. Bates, L. Spitzner, Ap.J. 113, 441 (1951).

[6] T.J. Millar, C.M. Leung, E. Herbst, Astron. Astrophys. 183, 109 (1987).

[7] R.I.Kaiser, Y.T. Lee, A.G. Suits, J. Chem. Phys. 103, 10395 (1995).

[8]. K. Roessler, H.J. Jung, B. Nebeling, Adv. Space. Res. **4**, 83 (1984).

[9]. K. Roessler, Rad. Eff. **99**, 21 (1986).

[10] E. Herbst, C.M. Leung, Ap.J. **233**, 170-180 (1990).

[11] M.M. Graff, Ap.J. **339**, 239-244 (1989).

[12] D.C. Clary, T.S. Stoecklin, A.G. Wickham, J. Chem. Soc. Far. Trans. **89**, 2185-2191 (1993).

[13] D.C. Clary, N. Haider, D. Husain, M.Kabir, Ap.J. **422**, 416-422 (1994).

[14] R.P.A. Bettens, H.H. Lee, E. Herbst, Ap.J. **443**, 664-674 (1995).

[15] R.P.A. Bettens, E. Herbst, E. Int. J. Mass Spectr. Ion. Proc. **149/150**, 321-343 (1995).

[16] E. Herbst, Lee, D.A. Howe, T.J. Millar, Month. Notice. Roy. Astron. Soc. **268**, 335-344 (1994).

[17] R.I.Kaiser, Y.T. Lee, A.G. Suits, J. Chem. Phys. (submitted).

[18] E.C. Sutton, R. Peng, W.C. Danchi, P.A. Jaminet, G. Sandell, A.P.G. Russel, Ap.J. Supl. Series 97, 455 (1995).

[19] F. Combes, G. Wlodarczak, P. Encrenaz, C. Laurent, Astron .Astrophys. 253, L29 (1992).

[20] A. Coustenis, B. Bezard, D. Gautier, A.MArten, R. Samuelson, Icarus 89, 152 (1989).

[21] C.R. Wu, T.S. Chien, G.S. Liu, D.L. Judge, J.J. Caldwell, J. Chem. Phys. 91, 272 (1991).

[22] R. Hannel et al. , Science, 212, 192 (1981).

[23] G.R. Gladstone, M. Allen, Y.L. Yung, Icarus 119, 1 (1996).

[24] D. Toublanc, J.P. Parisot, J. Brillet, D. Gautier, F. Raulin, C.P. McKay, Icarus 113, 2 (1995).

[25] R.I. Kaiser, K. Roessler, Ap. J. (submitted).

[26] M. Hausmann, K.H. Homann, Ber.Buns. Phys. Chem. 94, 1308 (1990).

[27] H. Wang, M. Frenklach, J.Phys. Chem. 98, 11465 (1994).

[28] S.P. Walsh, J. Chem. Phys. 103, 8544 (1995).

[29] J.A. Miller, C.F. Melius Comb. Flame 91, 21 (1992).

[30] R.P. Duran, V.T. Amorrbieta, A.J. Colussi, J. Phys. Chem. 92, 636 (1988).

[31] R.P. Duran, V.T. Amorrbieta, A.J. Colussi, Int. J. Chem. Kinetics, 21, 947 (1989).

[32] D.J. LeRoy, E.W.R. Steacie, J. Chem. Phys. 12, 117 (1944).

[33] M. Frenklach, D.W. Clary, W.C. Gardiner, in Proceedings of the 20th Symposium on

[34] M.B. Colket, Presented at the 21st Symposium on Combustion, Munich, 1986.

[35] Y. Hidaka, K. Tanaka, M. Suga, Chem. Phys. Let. 130, 190 (1986).

[36] W.C. Hung, M.L. Huang, Y.C. Lee, Y.P. Lee, J.Chem. Phys. 103, 9941 (1995).

[37] S.J. Harris, H.S. Shin, D.G. Goodwin, Appl. Phys. Let. 66, 891 (1995).

[38] T.K. Ha, E. Gey, J. Mol. Structure 306, 197 (1994).

[39] E. Gey, S. Wiegratz, W.Huehnel, B. Ondruschka, W. Saffert, G. Zimmermann, J. Mol. Structure 184, 69(1989).

[40] P.H. Kasai, L. Skattebol, E.B. Whipple, J. Am. Chem. Soc. 90, 4509 (1986).

[41] P.H. Kasai, J. Am. Chem. Soc. 94, 5950 (1972).

[42] A.L. Cooksy, J. Am. Chem. Soc. 117, 1098 (1995).

[43] W. Weng, T. Bartik, M.T. Johnson, A.M. Arif, J.A. Gladysz, Organometallics 14, 889 (1995).

[44] A.J. Arce, R. Machado, C. Rivas, Y. DeSanctis, J. Deeming, J. Organometallic Chemistry 419, 63 (1991).

[45] Y.T. Lee, J.D.McDonald, P.R.LeBreton, D.R. Herschbach,, Rev. Sci. Instr 40, 1402 (1969).

[46] R.I. Kaiser, A.G. Suits, Rev. Sci. Instr. 66, 5405-5410 (1995).

[47] G.O. Brink, Rev. Sci. Instr. 37, 857 (1966).

[48] N.R. Daly, Rev. Sci. Instr. 31, 264 (1960).

[49] J.M. Parson, K. Shobatake, Y.T. Lee, S.A. Rice, J. Chem. Phys. 59, 1402 (1973).

[50] M.S. Weis, Ph.D. thesis, University of California, Berkeley (1986).

[51] M. Vernon, LBL-Report 12422 (1981).

[52] Handbook of Chemistry and Physics, CRC Press, Boca Raton (1995).

[53] S. Walsh, NASA Ames Research Center, Moffet Field, private communication.

[54] W.B. Miller, S.A. Safron, D.R. Herschbach, Discuss. Faraday. Society 44, 108, 291 (1967).

[55] W.B. Miller, Ph.D. thesis, Harvard University, Cambridge (1969).

[56] D.C. Clary, N. Haider, D. Husain, M. Kabir, Ap.J. 422, 416 (1994).

[57] R.D. Levine, and R.B. Bernstein, Molecular Reaction Dynamics and Chemical Reactivity, Oxford University Press, Oxford (1987).

[58] J.O. Hirschfelder, C.F. Curtiss, R.B. Bird, Molecular Theory of Gases and Liquids, New York, Wiley (1954).

[59] J.M. Bofill, J. Farras, S. Olivella, A. Sole, J. Vilarrasa, J. Am. Chem. Soc. 110, 1694 (1988).

[60] G. Maier, H.P. Reisenauer, W. Schwab, P. Carsky, V. Spirsko, B.A.Hess, L.J. Schaad, J. Chem. Phys. 91, 4763 (1989).

[61] T.J. Lee, A. Bunge, H.F. Schaefer, J. Am. Chem. Soc. 107, 137 (1985).

[62] V. Jonas, M. Böhme, G. Frenking, J. Phys. Chem. 96, 1640 (1992).

[63] H. Clauberg, D.W. Minsek, P. Chen, J. Am. Chem. Soc. 114, 99 (1992).

[64] R. Herges, A. Mebel, J. Am. Chem. Soc. 116, 8229 (1994).

[65] W.J. Hehre, J.A. Pople, W.A. Lathan, L. Radom, E. Wasserman, Z.R. Wasserman, J. Am. Chem. Soc. 98, 4378 (1976).

[66] M. Marshall, Ph.D. thesis, Yale Unversity.

[67] S.S. Shaik, E. Canadell, J.Am. Chem. Soc. 112, 1446 (1990).

[68] R.I. Kaiser, Y.T. Lee, A.G. Suits, unpublished.

[69] R.I. Kaiser, D. Stranges, Y.T. Lee, A.G. Suits, to be submitted to J. Chem. Phys..

Fig. 1. Structures of low lying C_4H_3 isomers as well as metalated radicals M1 and M2. A linear isomer of (4), analogous to the c/l-C_3H isomer pair, has not been investigated. Since c- and l-C_3H differ only by 8 ± 4 kJmol^{-1}, the linear isomer (5) holds approximately Δ_fH = 560 kJmol^{-1}. Other enthalpies of formations for the isomers are (1) 486, (2) 526, (3) 541, (4) 553, (6) 572, (7) 604, (8) 613, (9) 660, and (10) 766 kJmol^{-1}.

Fig. 2. Lower: Newton diagram for the reaction $C(^3P_j)$ + $CH_3CCH(X^1A_1)$ at a collision energy of 20.4 kJmol^{-1}. The circles stand for the maximum center-of-mass recoil velocity. From outer to inner: n-C_4H_3, i-C_4H_3, C_4H_3 isomers (3)-(8, and C_4H_3 isomer (9). Upper: Laboratory angular distribution of product channel at m/e = 51. Circles and 1σ error bars indicate experimental data, the solid lines the calculated distribution for the upper and lower carbon beam velocity (Tab. 1). C.M. designates the center-of-mass angle. The solid lines originating in the Newton diagram point to distinct laboratory angles whose TOFs are shown in Fig. 4.

Fig. 3. Lower: Newton diagram for the reaction $C(^3P_j)$ + $CH_3CCH(X\ ^1A_1)$ at a collision energy of 33.2 kJmol^{-1}. The circles are corrected for difference in the relative collision energy. Upper: Laboratory angular distribution of product channel at m/e = 51. Circles and 1σ error bars indicate experimental data, the solid lines the calculated distribution for the upper and lower carbon beam velocity. The solid lines originating in the Newton diagram point to distinct laboratory angles whose TOFs are shown in Fig. 5.

Fig. 4. Time-of-flight data at m/e = 51 for laboratory angles 35, 40, 45, 50, 55, and 60°at a collision energy of 20.4 kJmol^{-1}. Open circles represent experimental data, the solid line the fit. TOF spectra have been normalized to the relative intensity at each angle.

Fig. 5. Time-of-flight data at m/e = 51 for indicated laboratory angles at a collision energy of 33.2 kJmol^{-1}. Open circles represent experimental data, the solid line the fit. TOF spectra have been normalized to the relative intensity at each angle.

Fig. 6. Lower: Center-of-mass angular flux distribution for the reaction $C(^3P_j)$ + $CH_3CCH(X^1A_1)$ at a collision energy of 20.4 kJmol^{-1}. Upper: Center-of-mass translational energy flux distribution for the reaction $C(^3P_j)$ + $CH_3CCH(X^1A_1)$ at a collision energy of 20.4 kJmol^{-1}. Dashed and solid lines limit the range of acceptable fits within 1σ error bars.

Fig. 7. Lower: Center-of-mass angular flux distribution for the reaction $C(^3P_j)$ + $CH_3CCH(X^1A_1)$ at a collision energy of 33.2 kJmol^{-1}. Upper: Center-of-mass translational energy flux distribution for the reaction $C(^3P_j)$ + $CH_3CCH(X^1A_1)$ at a collision energy of 33.2 kJmol^{-1}. Dashed and solid lines limit the range of acceptable fits within 1σ error bars.

Fig. 8. Contour flux map for the C_4H_3 product from the reaction $C(^3P_j)$ + $CH_3CCH(X^1A_1)$ at a collision energy of 20.4 kJmol^{-1}.

Fig. 9. Contour flux map for the C_4H_3 product from the reaction $C(^3P_j)$ + $CH_3CCH(X^1A_1)$ at a collision energy of 33.2 kJmol^{-1}.

Fig. 10. Principal rotation axis of the butatrienyl radical. The C-axis is perpendicular to the paper plane.

Fig. 11. A) Schematic representation of the lowest energy pathways on the triplet C_4H_4 PES, structures of potentially involved collision complexes, and their enthalpies of formation. Triplet methylenecyclopropene and vinylacetylene are not included, since their singlet-triplet gaps have not been investigated yet. B) Additional structures for possible intermediates and products relevant to the discussion. Three potential electronic structures of propargylene are presented: 1,3-diradical (16a) and carben-like structures (16b/c).

Fig. 12. Approach geometry of the carbon atom toward the methylacetylene molecule conserving C_s symmetry and induced rotation around the B-axis.

Tab. 1: Experimental beam conditions and 1σ errors averaged over the experimental time: most probable velocity v_0, speed ratio S, most probable relative collision energy, E_{coll}, center-of-mass angle, θ_{CM}, composition of the carbon beam, and flux factor $f_v = n(C) * n(C_3H_4) * v_r$ in relative units, with the number density of the ith reactant n_i and the relative velocity v_r.

beam	v_0, ms^{-1}	S	E_{coll}, $kJmol^{-1}$	θ_{CM}	$C_1:C_2:C_3$	f_v
$C(^3P_j)$/Ne	1950 ± 40	3.9 ± 0.3	20.4 ± 1.0	53.5 ± 1.5	1:0.6:0.7	1.0
$C(^3P_j)$/He	2560 ± 50	4.7 ± 0.3	33.2 ± 1.4	46.2 ± 1.6	1:0.4:0.9	1.8 ± 0.3
C_3H_4	790 ± 30	7.7 ± 0.5	-	-	-	-

Tab. 2: Thermochemistry of the reaction $C(^3P_j) + CH_3CCH(X^1A_1)$. Enthalpies of formations were taken from references [28, 38, 39, 52, 53]. The symmetry of the n-C_4H_3 ground state electronic wave function is omitted.

#	exit channel	free reaction enthalpy at 0 K, $\Delta_R H(0\ K)$, $kJmol^{-1}$
1	n-C_4H_3 (?) + H ($^2S_{1/2}$)	-194 ± 1
2	HCCCCH ($X^1\Sigma_g^+$) + H_2 ($X^1\Sigma_g^+$)	-444 ± 12
3	HCCCCH ($X^1\Sigma_g^+$) + 2 H ($^2S_{1/2}$)	-12 ± 12
3	C_4H ($X^2\Sigma$) + H_2 ($X^1\Sigma_g^+$) + H ($^2S_{1/2}$)	+ 78 ± 10
4	C_4 ($X^3\Sigma_g^-$) + 2 H_2 ($X^1\Sigma_g^+$)	+ 68 ± 15
5	C_3H_3 (X^2B_1) + CH ($X^2\Pi$)	+ 35 ± 12
6	c-C_3H_2 (X^1A_1) + CH_2 (X^3B_1)	- 22 ± 5
7	c-C_3H (X^2B_1) + CH_3 (X^2A_2'')	- 36 ± 4
8	l-C_3H ($X^2\Pi$) + CH_3 (X^2A_2'')	- 28 ± 4
9	C_3 ($X^1\Sigma_g^+$) + CH_4 (X^1A_1)	- 151.5 ± 1
10	C_2H_4 (X^1A_g) + C_2 ($X^1\Sigma_g^+$)	- 6 ± 1
11	C_2H_3 (X^2A') + C_2H ($X^2\Sigma^+$)	- 30 ± 6
12	C_2H_2 ($X^1\Sigma_g^+$) + C_2H_2 ($X^1\Sigma_g^+$)	- 440 ± 1

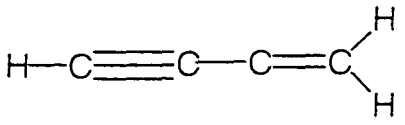

(1a)

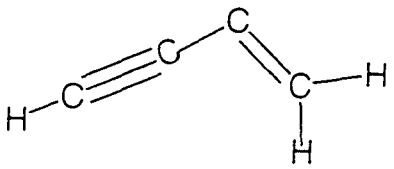

(1b)

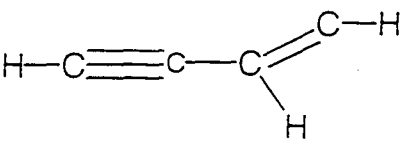

(2)

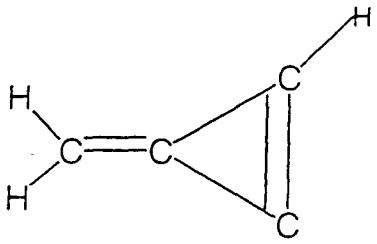

(3)

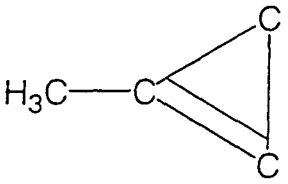

(4)

(5)

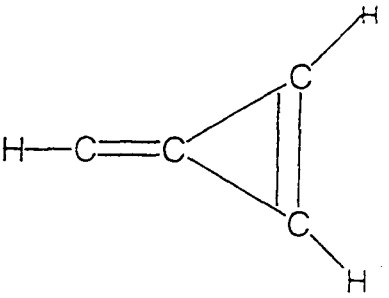

(6)

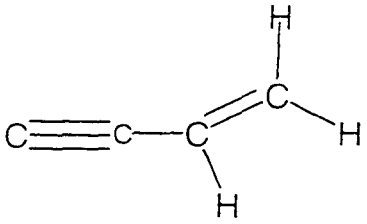

(7)

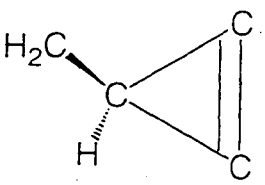

(8)

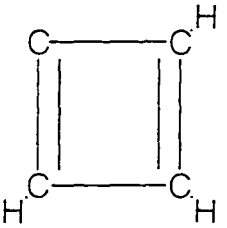

(9)

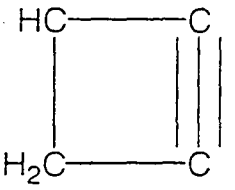

(10)

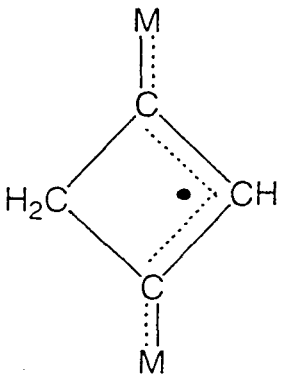

(M1)

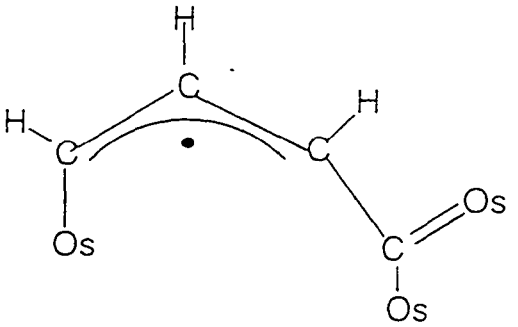

(M2)

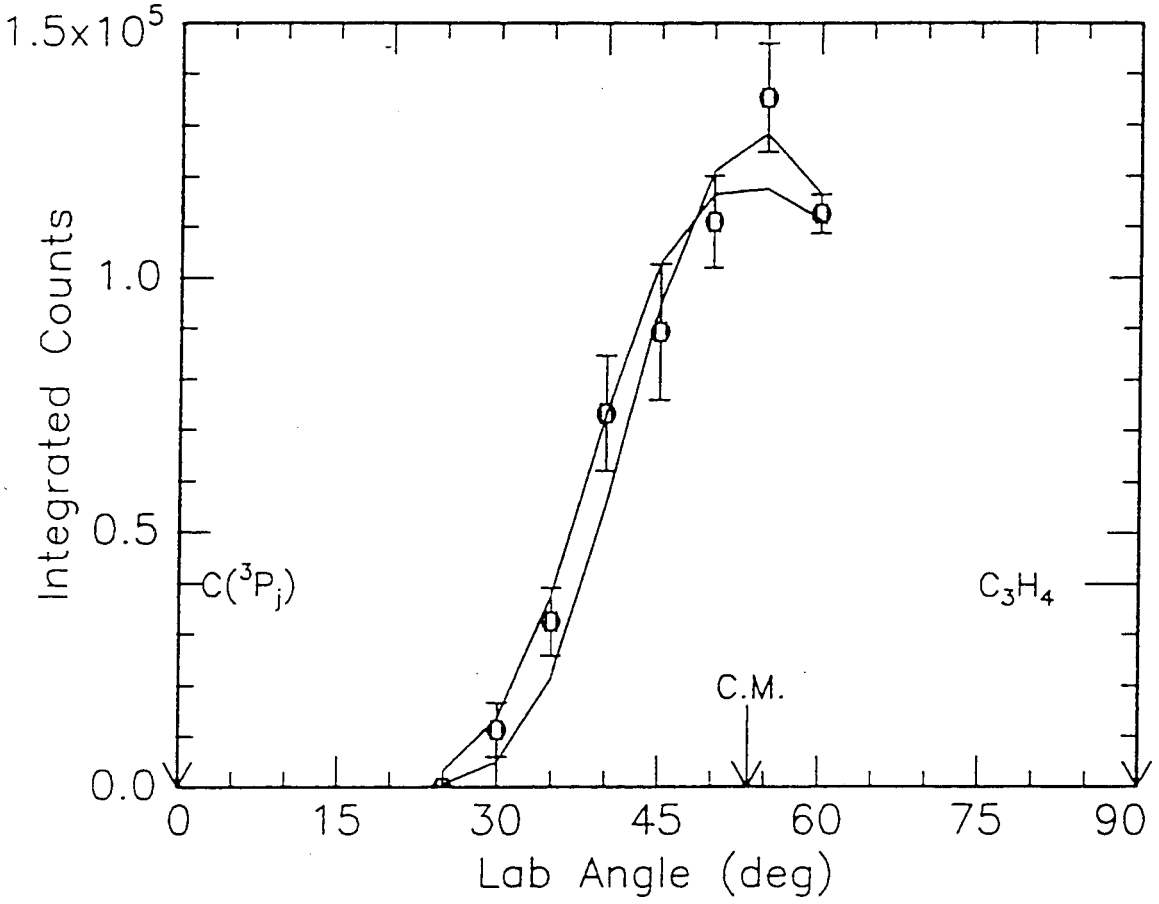
1.5x10^5
1.0
0.5
0.0
Integrated Counts
C(3Pj)
C3H4
C.M.
0
15
30
45
60
75
90
Lab Angle (deg)

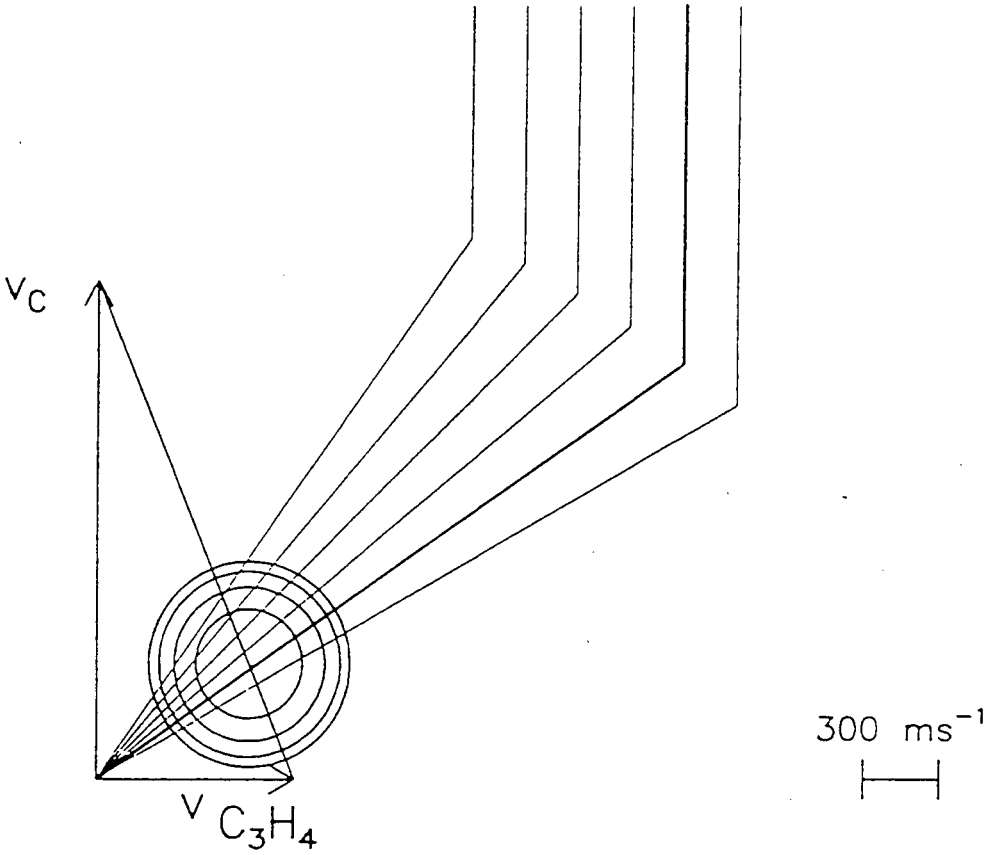
vC
v C3H4
300 ms-1

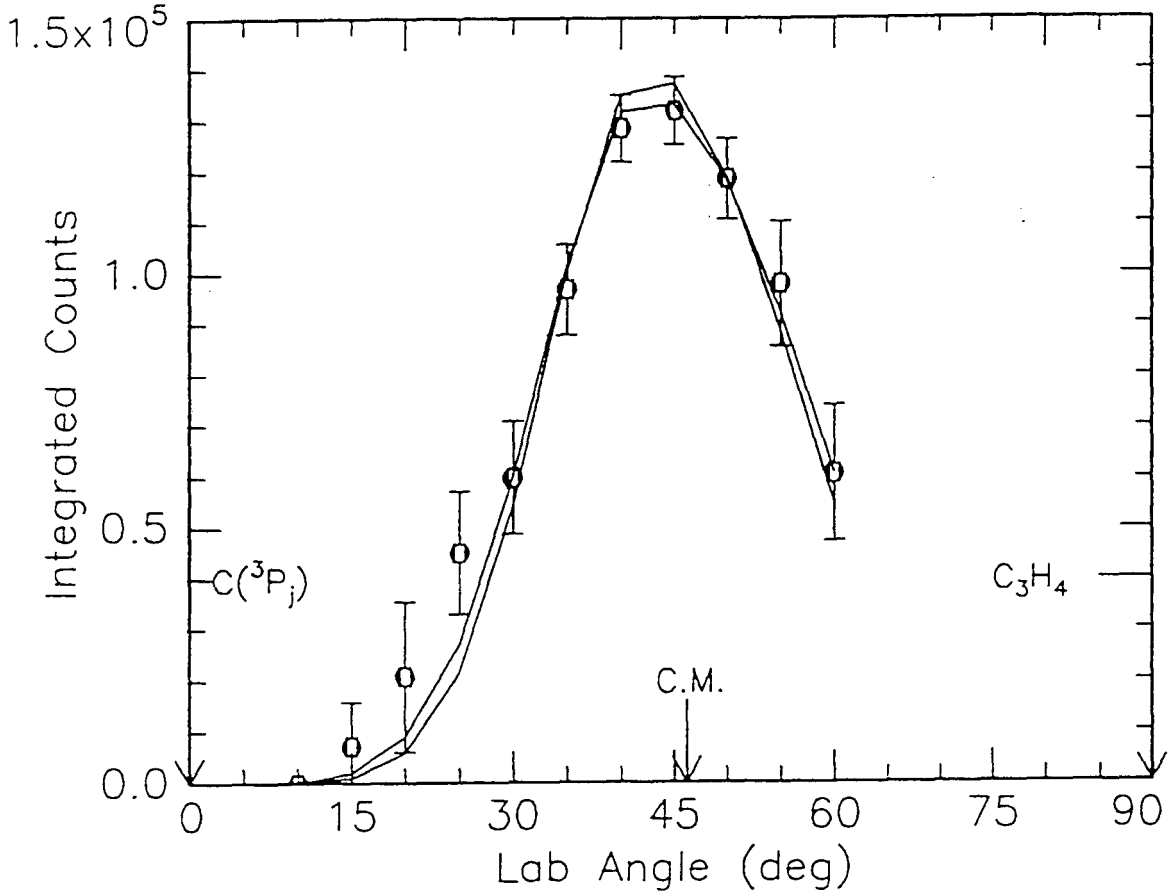
1.5x10^5
1.0
0.5
0.0
Integrated Counts
C(3Pj)
C3H4
C.M.
0
15
30
45
60
75
90
Lab Angle (deg)

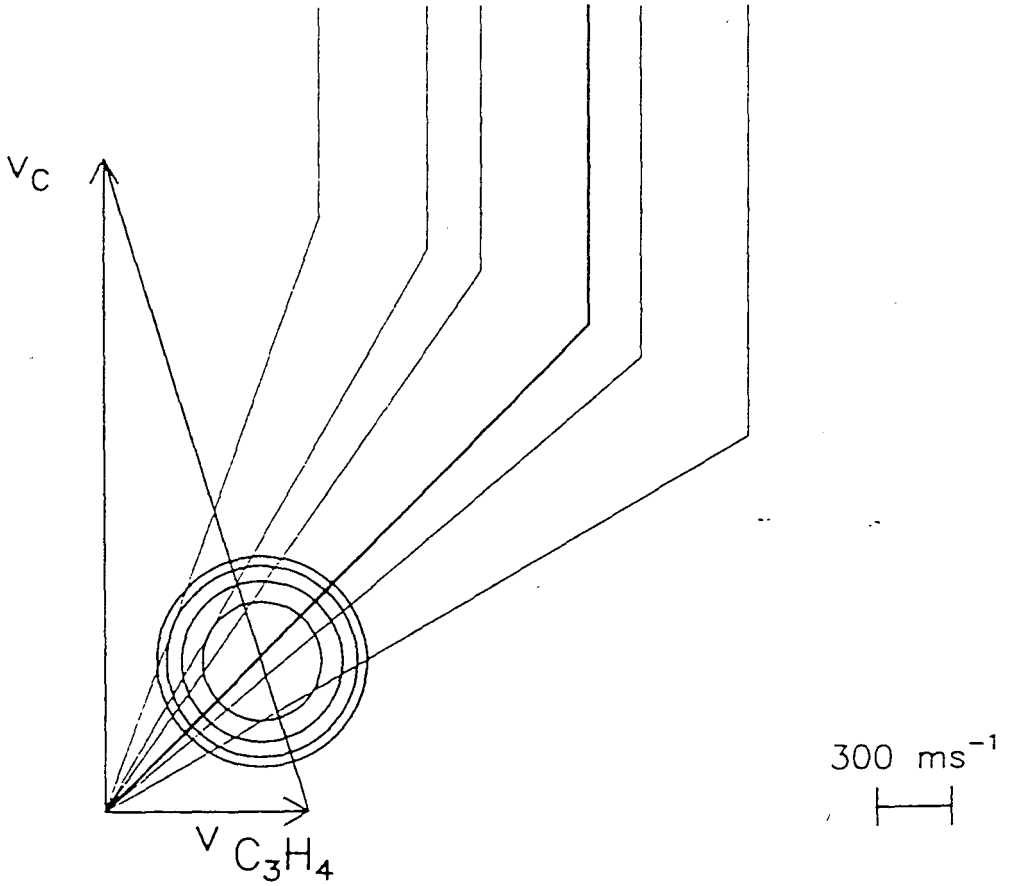
vC
v C3H4
300 ms-1

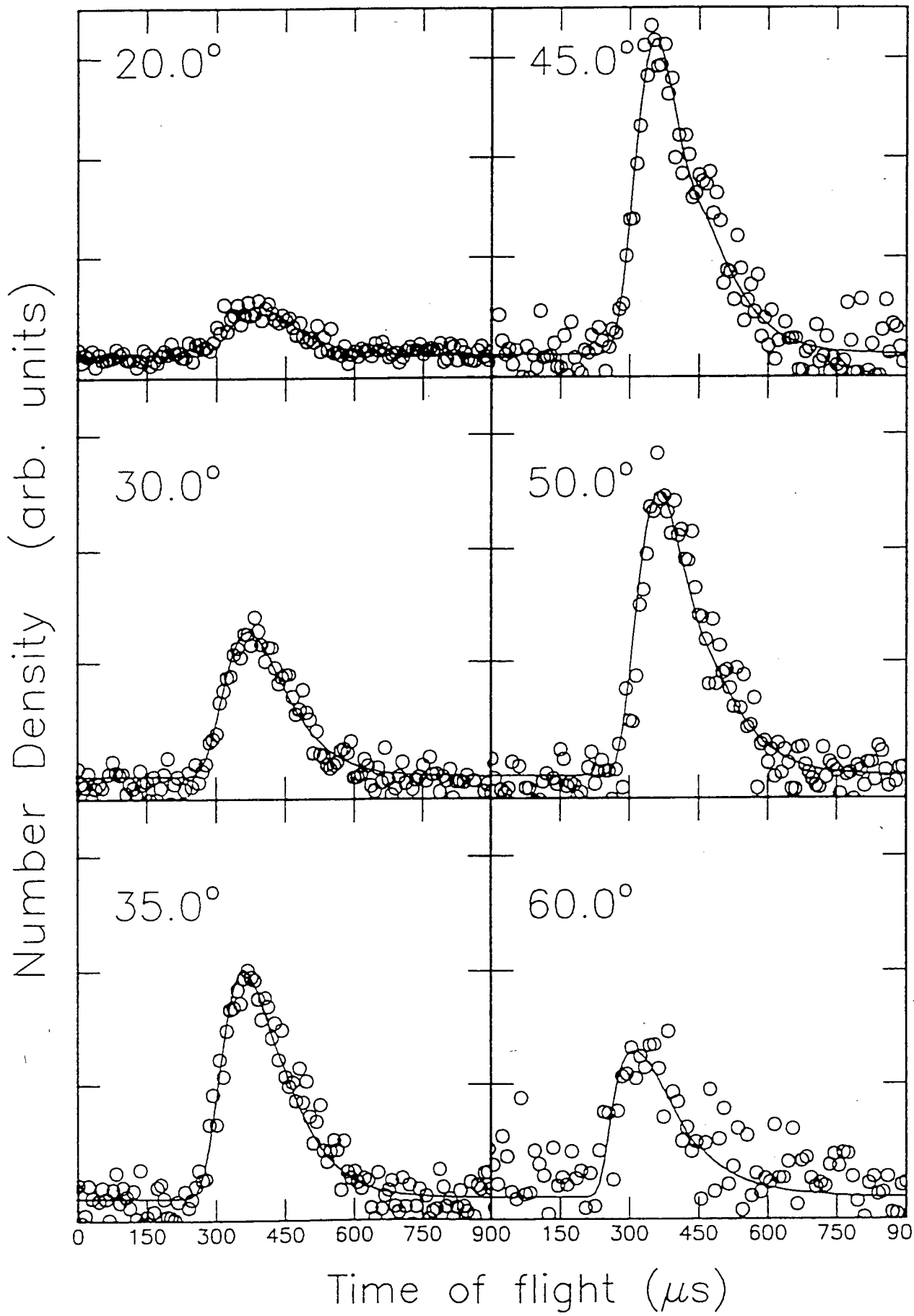
20.0°
45.0°
30.0°
50.0°
35.0°
60.0°
Number Density (arb. units)
0
150
300
450
600
750
900
150
300
450
600
750
900
Time of flight (μs)

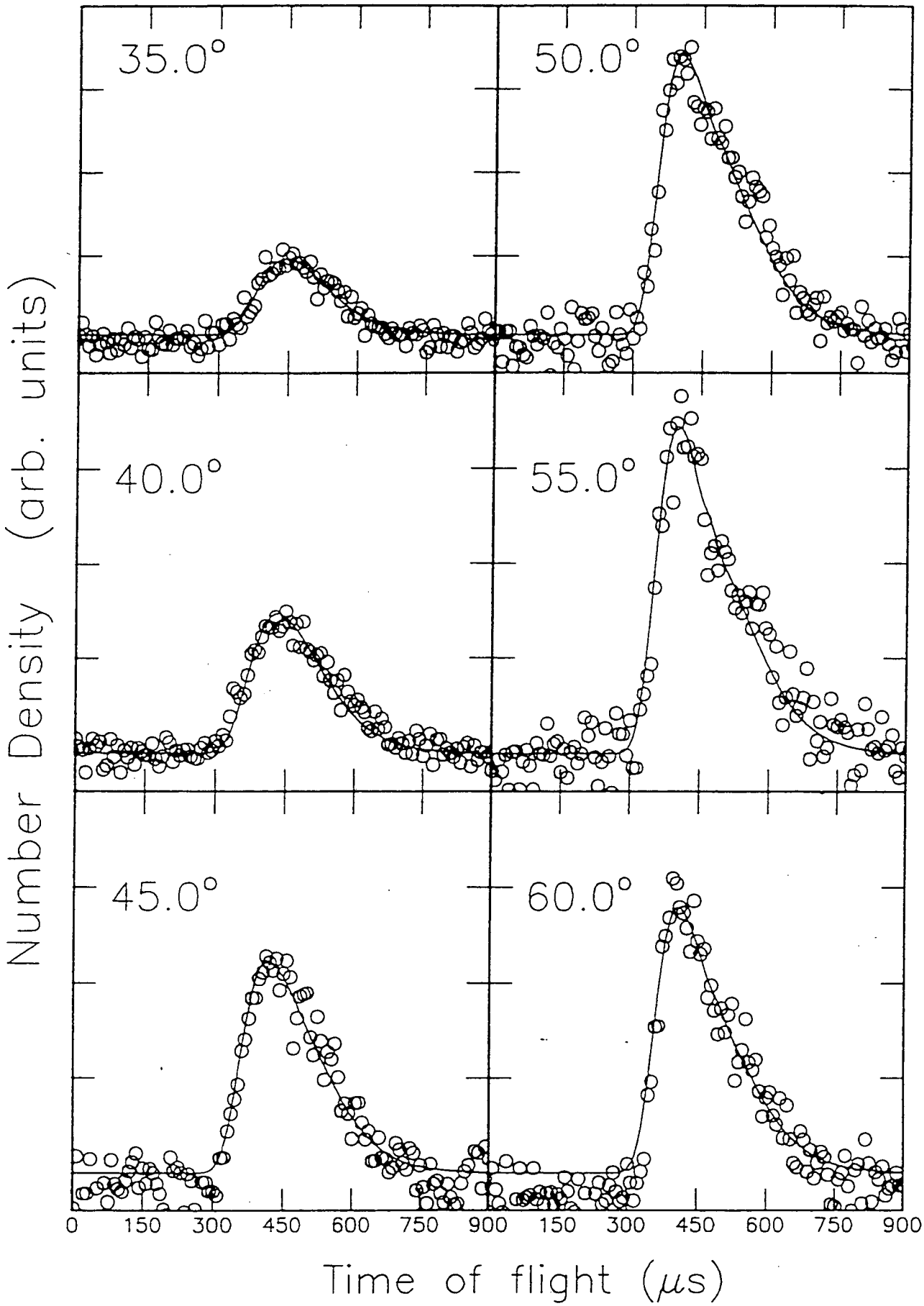
35.0°
50.0°
40.0°
55.0°
45.0°
60.0°
Number Density (arb. units)
0
150
300
450
600
750
900
Time of flight (μs)

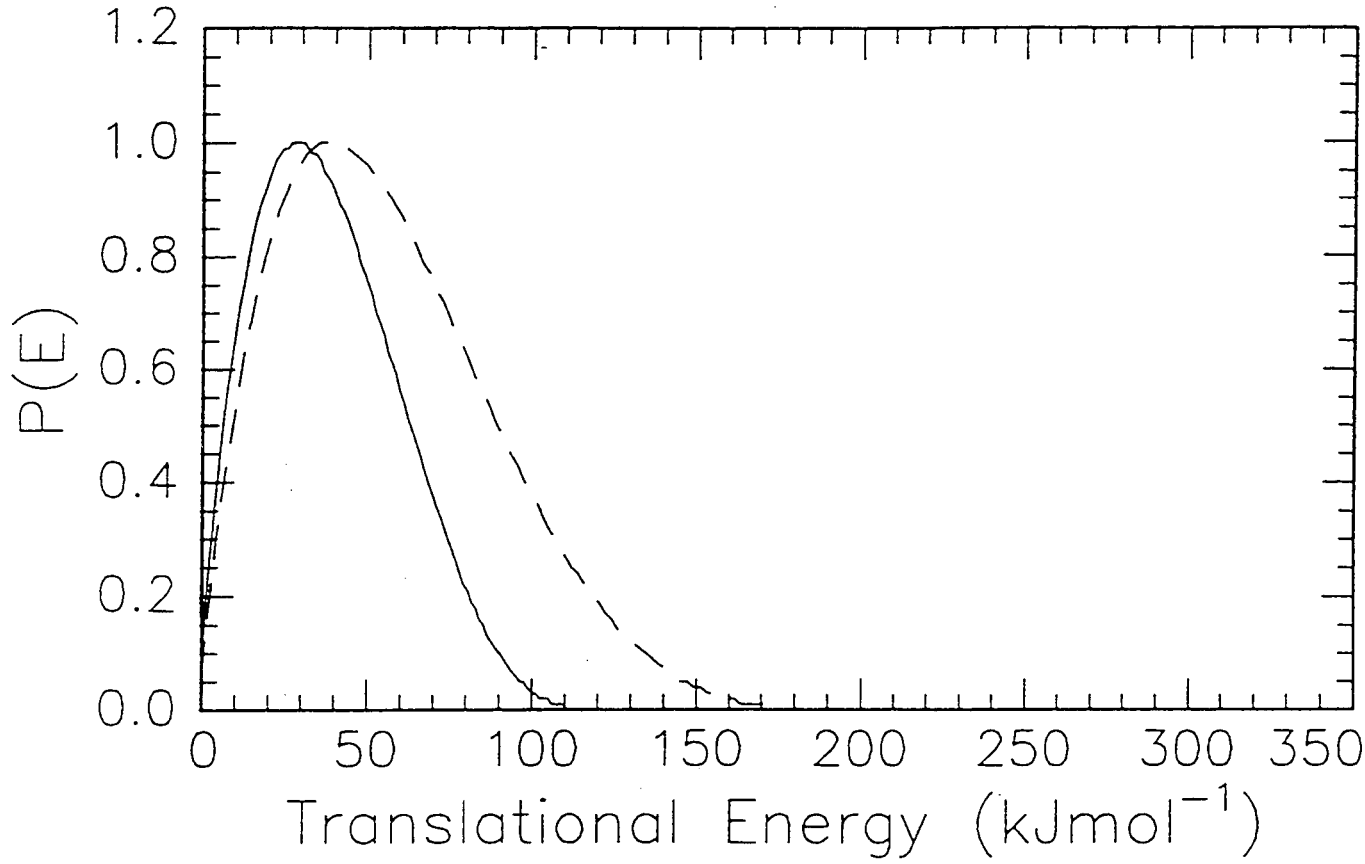
1.2
1.0
0.8
0.6
0.4
0.2
0.0
P(E)
0
50
100
150
200
250
300
350
Translational Energy (kJmol^{-1})

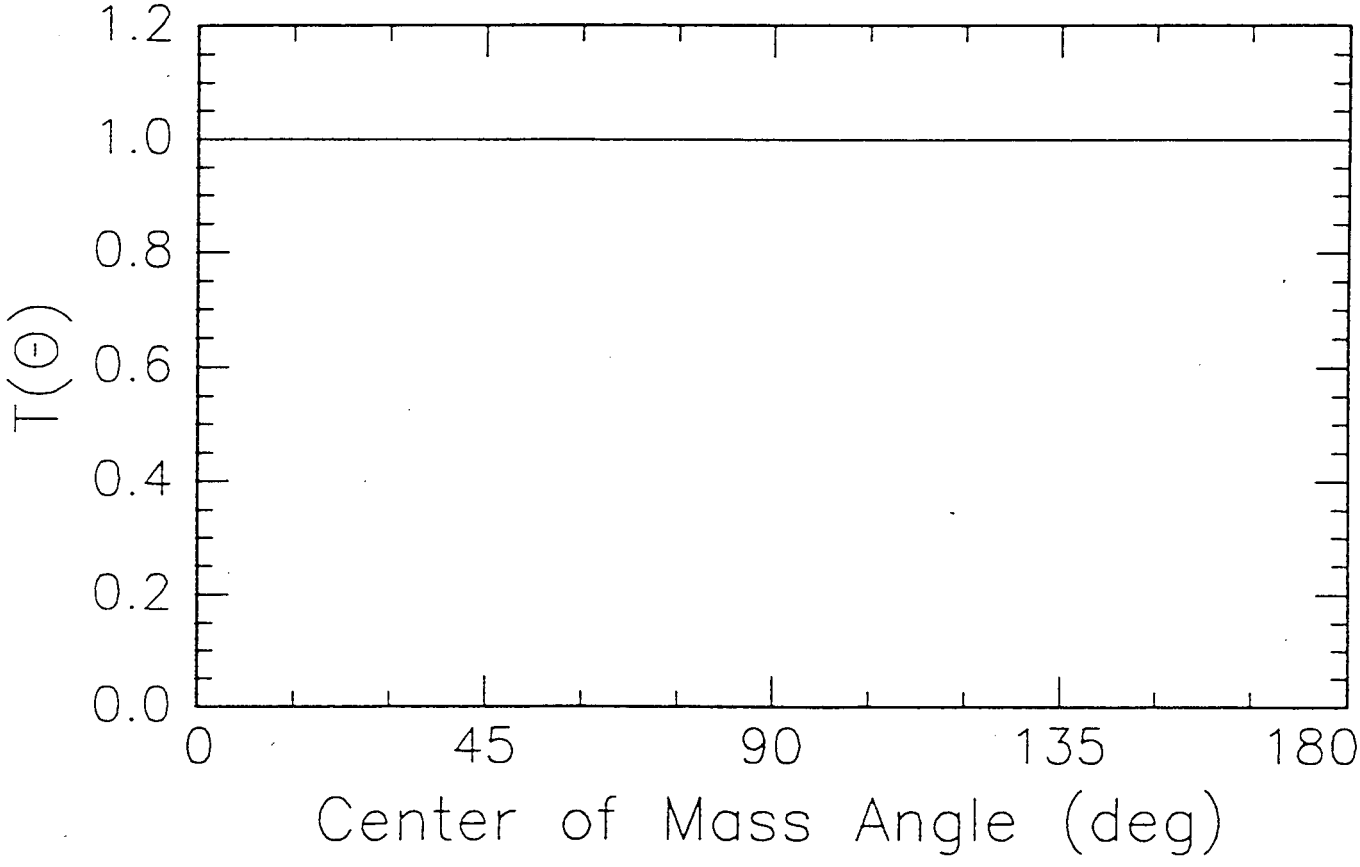
1.2
1.0
0.8
0.6
0.4
0.2
0.0
T(Θ)
0
45
90
135
180
Center of Mass Angle (deg)

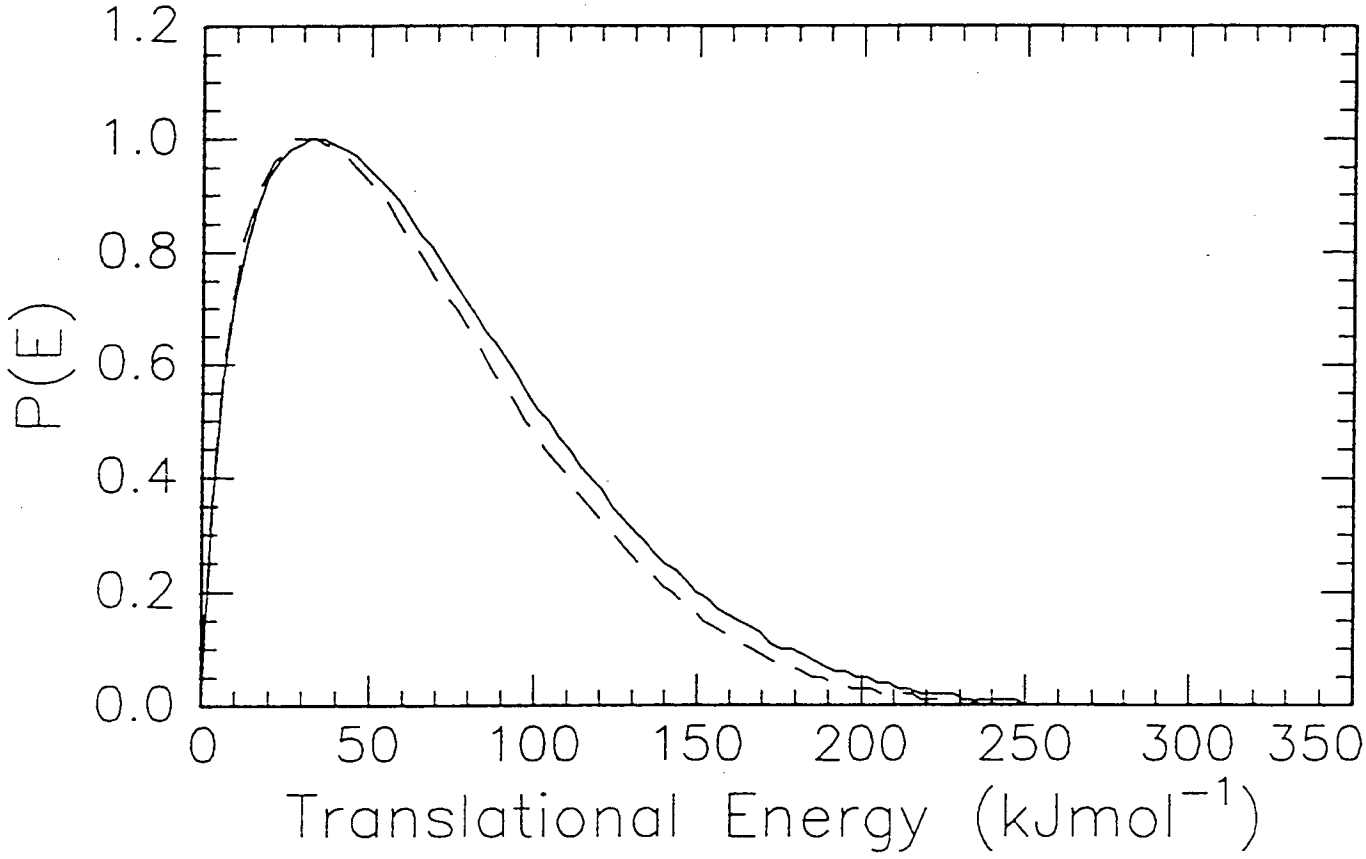
1.2
1.0
0.8
0.6
0.4
0.2
0.0
P(E)
0
50
100
150
200
250
300
350
Translational Energy (kJmol^{-1})

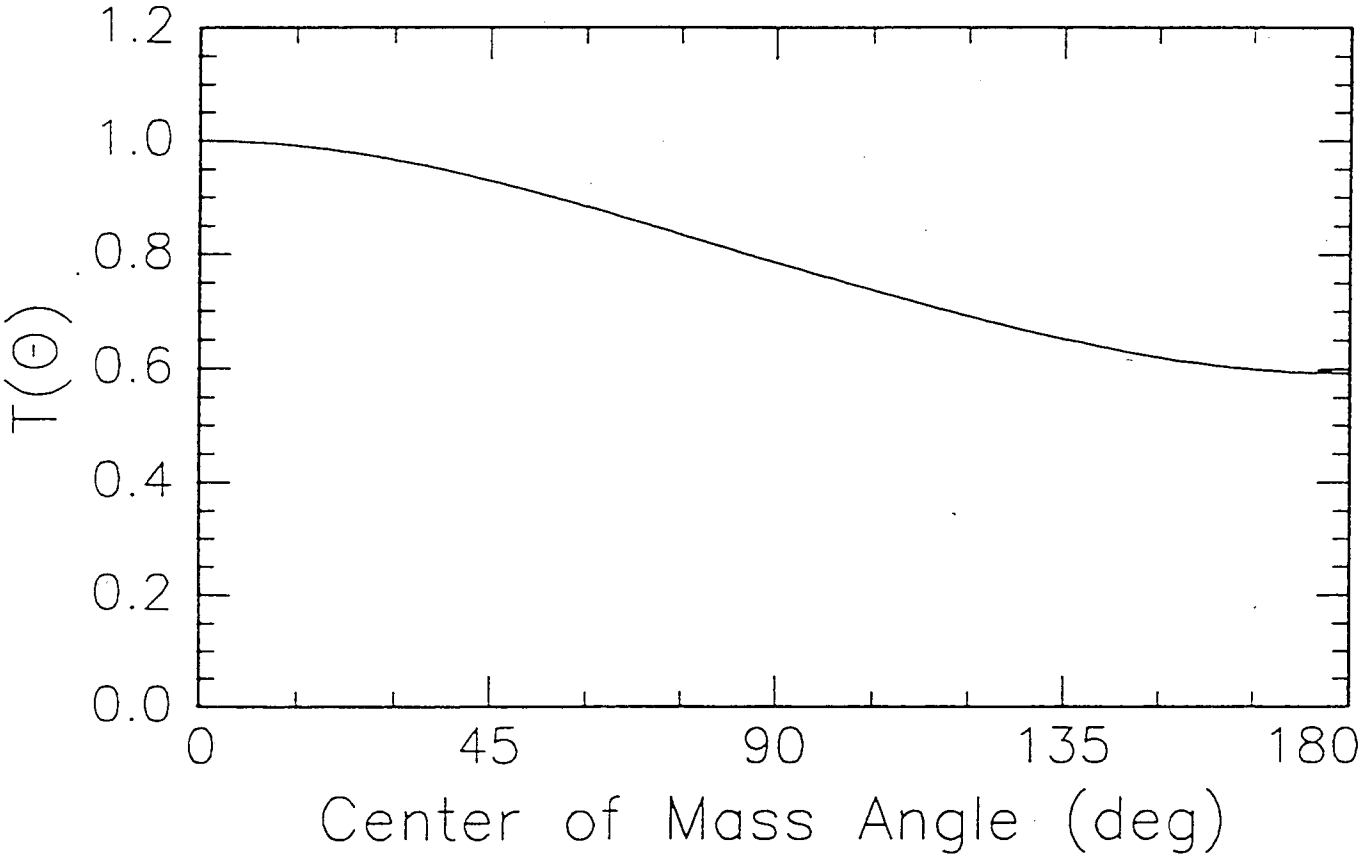
1.2
1.0
0.8
0.6
0.4
0.2
0.0
T(Θ)
0
45
90
135
180
Center of Mass Angle (deg)

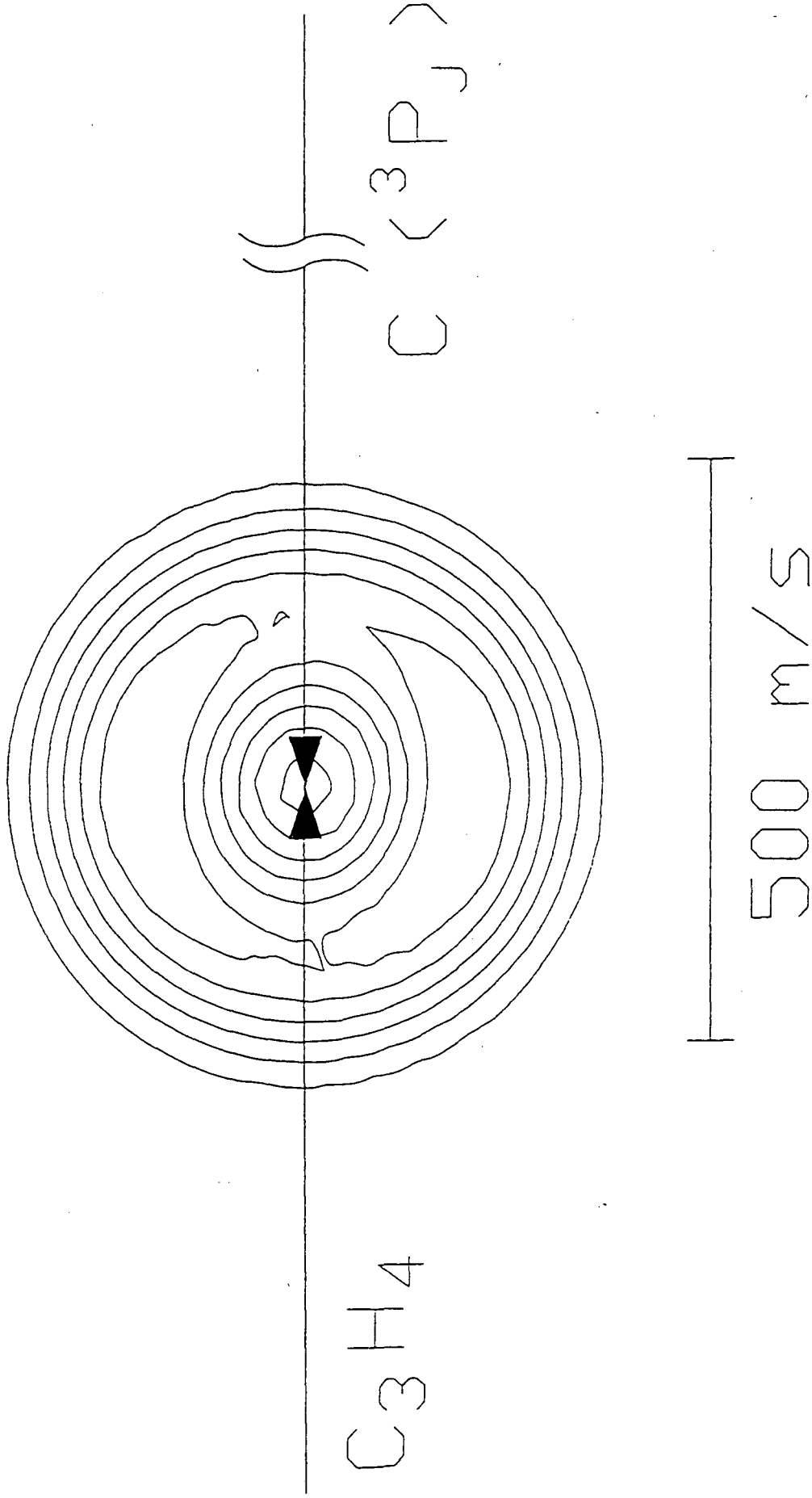
C (3PJ)
500 m/s
C3H4

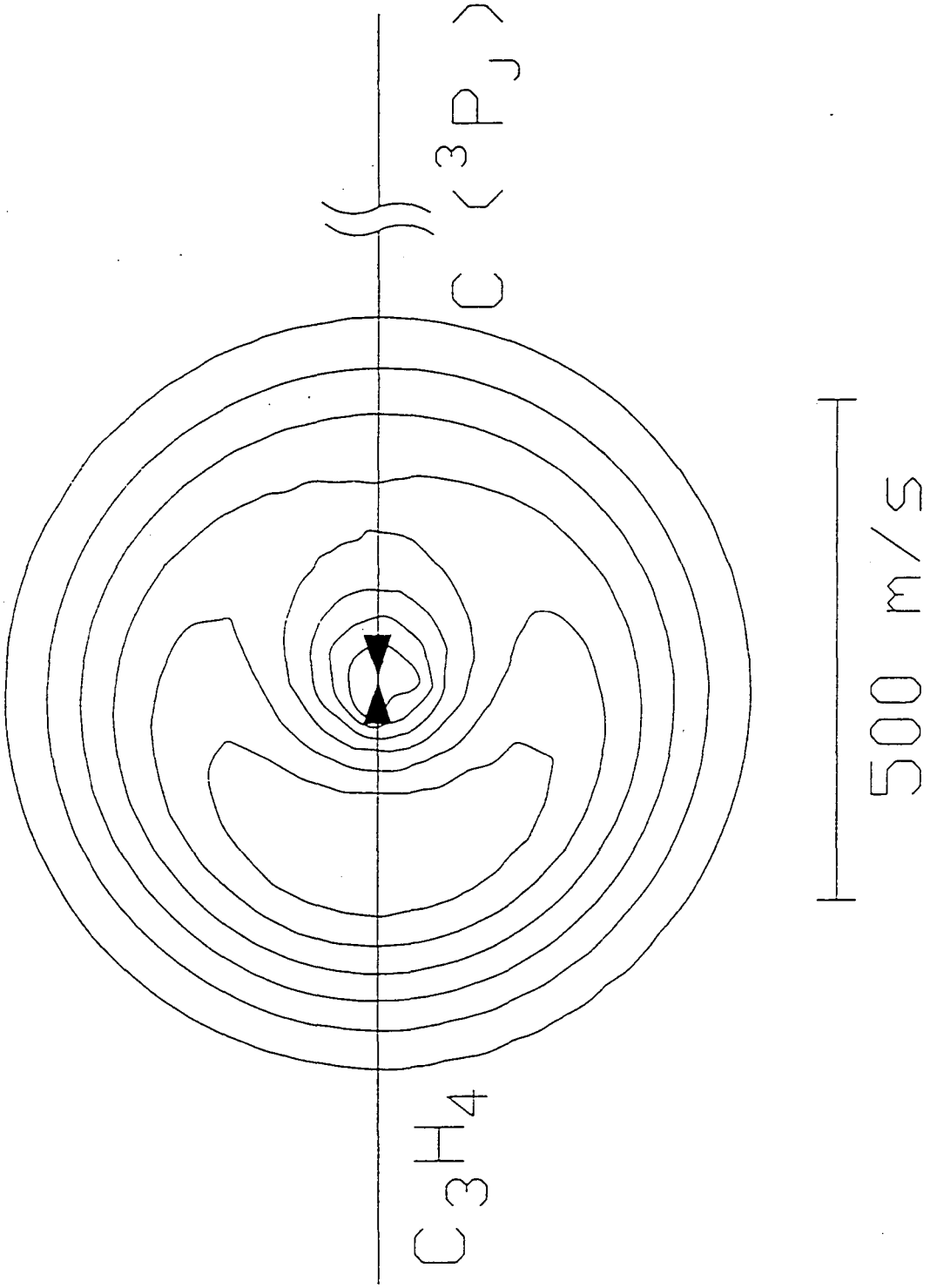
C (3 P J)
C 3 H 4
500 m/s

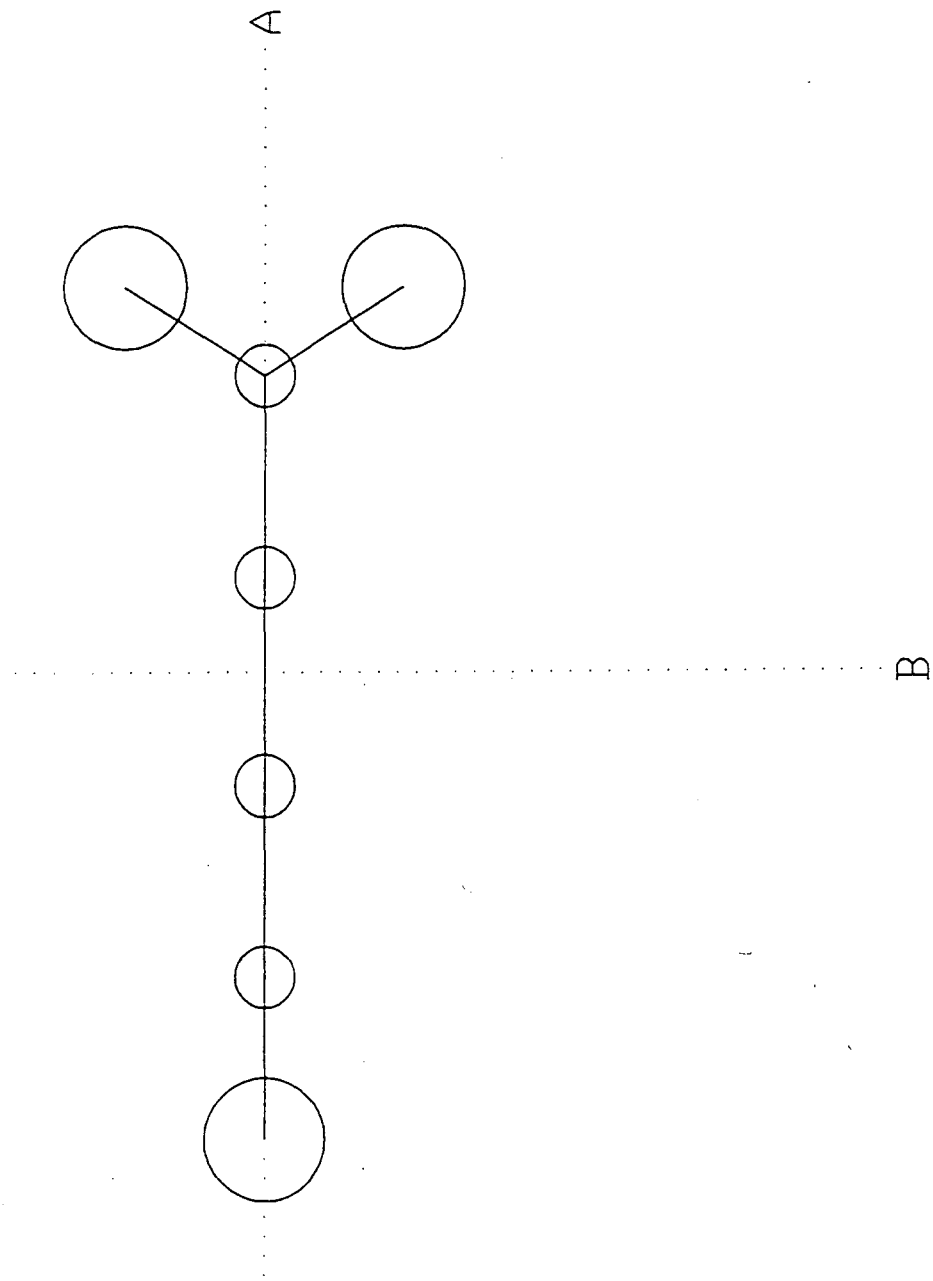
A
B

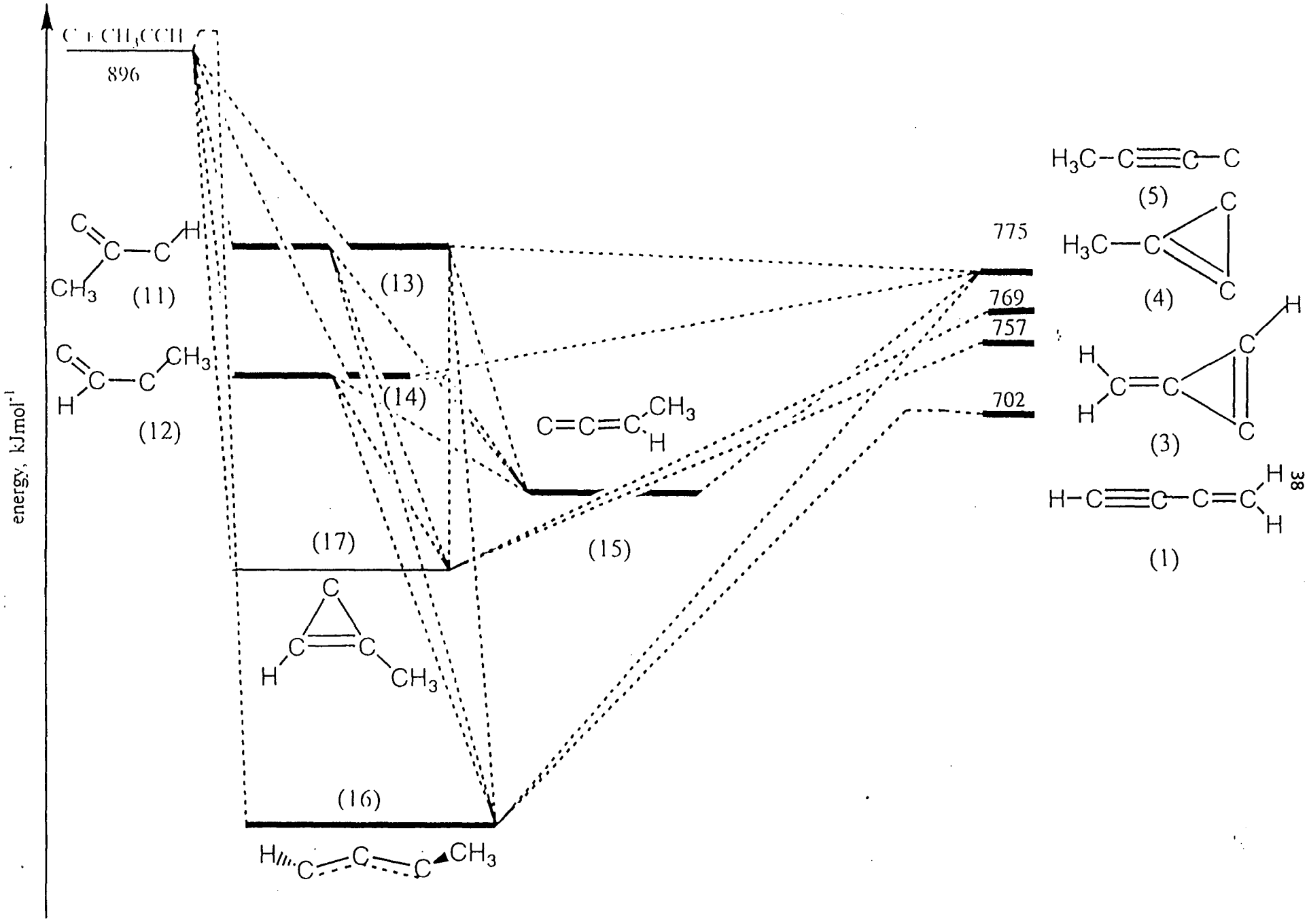
energy, kJmol-1
896
(11)
(12)
(13)
(14)
(15)
(16)
(17)
775
769
757
702
(5)
(4)
(3)
(1)

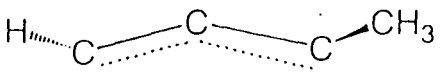

(16a)

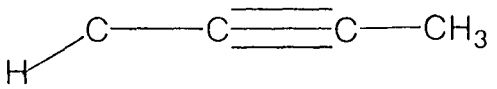

(16b)

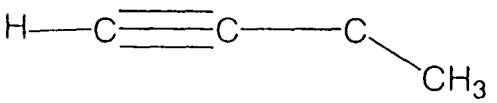

(16c)

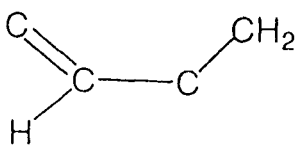

(18)

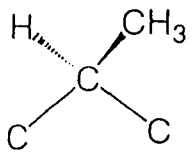

(19)

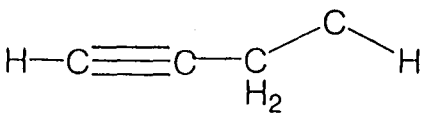

(20)

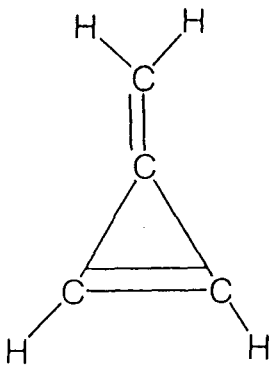

(21)

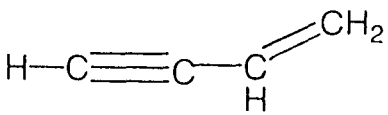

(22)

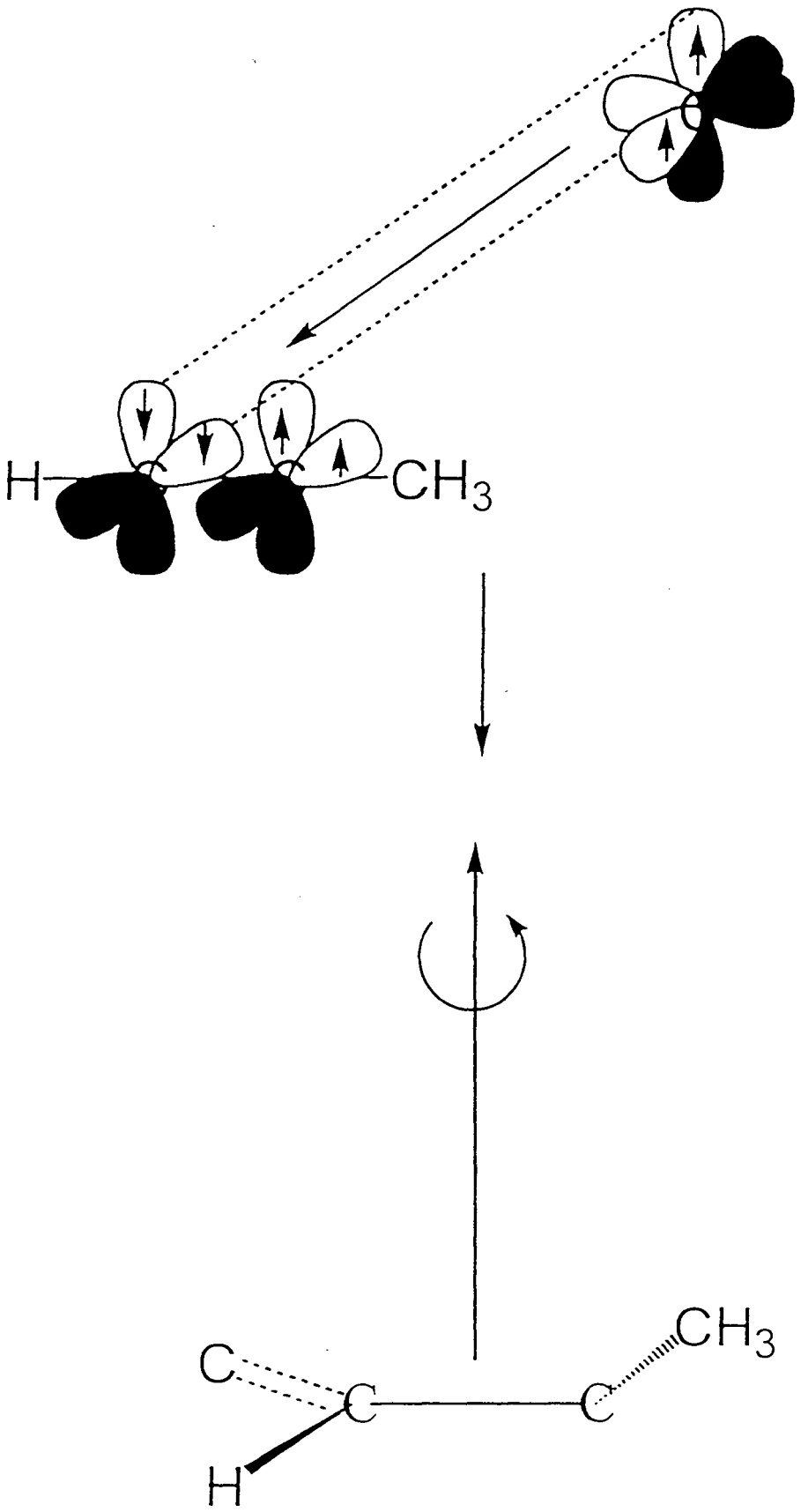
H
CH3
C
C
C
CH3
H

Ernest Orlando Lawrence Berkeley National Laboratory
One Cyclotron Road | Berkeley, California 94720

Prepared for the U.S. Department of Energy under Contract No. DE-AC03-76SF00098